Developmental Biology **216,** 114–134 (1999)
Article ID dbio.1999.9471, available online at http://www.idealibrary.com on IDEAL®

Organogenesis of the *Caenorhabditis elegans* Intestine

Ben Leung,*,†,[1] Greg J. Hermann,*,§,[1] and James R. Priess*,†,‡,§,[2]

**Division of Basic Sciences, Fred Hutchinson Cancer Research Center, Seattle, Washington 98109; †Molecular and Cellular Biology Program and ‡Department of Zoology, University of Washington, Seattle, Washington 98195; and §Howard Hughes Medical Institute, Seattle, Washington 98109*

The intestine of *Caenorhabditis elegans* is an epithelial tube consisting of only 20 cells and is derived clonally from a single embryonic blastomere called E. We describe the cellular events that shape the intestine. These events include cytoplasmic polarization of cells in the intestinal primordium, the intercalation of specific sets of cells, the generation of an extracellular cavity within the primordium, and adherens junction formation. The polarization of the intestinal primordium is associated with the generation of an asymmetric microtubule cytoskeleton, and microtubule function plays a role in subsequent cell polarity. We show that an isolated E blastomere is capable of generating polarized intestinal cells, indicating that some of the major events in intestinal organogenesis do not depend upon interactions with surrounding tissues. We compare and contrast intestinal organogenesis with some of the basic steps in development of a second epithelial organ, the pharynx, and suggest how these differences lead to organs with distinct shapes.

Key Words: **adherens junctions; *C. elegans;* cell polarity; centrosomes; epithelia; organogenesis; intercalation; intestine; microtubules; pharynx.**

INTRODUCTION

The development of the intestine has been a major focus of research on the *Caenorhabditis elegans* embryo. By the eight-cell stage of embryogenesis, one blastomere called E is specified to produce all of the intestinal cells and only intestinal cells (Sulston *et al.*, 1983). The early embryo is now known to contain asymmetrically localized, maternally provided factors that promote, or prevent, the intestinal cell fate (Schnabel and Priess, 1997; Bowerman, 1998; Labouesse and Mango, 1999). Further specification occurs through cell–cell interactions by a Wnt or Wingless-like signaling pathway (Lin *et al.*, 1995; Rocheleau *et al.*, 1997; Thorpe *et al.*, 1997). In response to these early events, the E blastomere expresses new transcription factors, such as the GATA-like factor END-1, that promote intestinal development (Zhu *et al.*, 1997; Newman-Smith and Rothman, 1998). Ectopic, heat shock-driven expression of END-1 can cause most or all embryonic cells to express intestine-specific genes and form structures with some of the characteristics of a normal intestine (Zhu *et al.*, 1998).

Although we have the beginning of a molecular picture for how the intestinal progenitor, E, becomes different from other early blastomeres, almost nothing is known about the downstream events that must be initiated by factors like END-1 to result in intestine-specific morphogenesis. The intestine, the pharynx, and the hypodermis are the three major epithelial organs in *C. elegans*. These epithelia form the cellular interface between the interior of the animal and the external environment. Each epithelial cell has an apical surface bordered by adherens junctions and a distinct basal surface associated with a basement membrane. Despite these and other common features, epithelial cells in the intestine must have unique morphogenetic properties that allow them to form a tube, rather than a sheet like the hypodermis or a cyst/tube like the pharynx.

Organ morphogenesis requires that cells become polarized and that this polarized state is coordinated between different cells. Studies on yeast and systems such as the early *C. elegans* embryo have provided insight into how single cells can exploit both intrinsic and extrinsic cues to become polarized, and have identified several genes

[1] These authors contributed equally to this work.

[2] To whom correspondence should be addressed. E-mail: jpriess@fred.fhcrc.org.

0012-1606/99 $30.00

that function in generating polarity (Chant, 1996; Guo and Kemphues, 1996; Madden and Snyder, 1998). For example, polarity in the newly fertilized *C. elegans* egg is mediated by a group of asymmetrically localized, cortical proteins collectively called PAR proteins (Kemphues and Strome, 1997; Bowerman and Shelton, 1999). Much of our current understanding about how epithelial cells become polarized during organogenesis has come from studies on vertebrate cells in culture. Results from several studies have suggested that cadherin-mediated cell–cell interactions and integrin-mediated cell–basement membrane interactions play critical roles in morphogenesis (Rodriguez-Boulan and Nelson, 1989; Eaton and Simons, 1995; Drubin and Nelson, 1996; Yeaman *et al.*, 1999). Genetic studies in mice, *Drosophila,* and *C. elegans* have begun to examine the roles of cadherins, integrins, and basement membrane components in the context of normal embryonic development. In *C. elegans,* mutations have been identified in the cadherins *hmr-1* and *cdh-3* (Pettitt *et al.*, 1996; Costa *et al.*, 1998), the three β-catenins (Rocheleau *et al.*, 1997; Costa *et al.*, 1998; Eisenmann *et al.*, 1998), the single α-catenin (Costa *et al.*, 1998), the two α-integrins and single β-integrin (Francis and Waterston, 1985; Gettner *et al.*, 1995; Baum and Garriga, 1997), and the genes encoding several components of the basement membrane such as type IV collagen (Graham *et al.*, 1997; Gupta *et al.*, 1997) and perlecan (Moerman *et al.*, 1996). Some of these genes apparently play a role in maintaining the cytoskeletal organization of polarized epithelial cells that are subjected to mechanical stress (see Costa *et al.*, 1998). However all of the mutants described thus far have tissues and organs with apparently normal epithelial organization. For example, all of these mutants appear to develop an intestine with clear apical–basal polarity.

These studies raise the question of whether epithelial polarity in *C. elegans* is generated by factors that individually have redundant or minor roles or whether there are other genes that have major roles in the generation and coordination of epithelial polarity that have not yet been described. It should be possible to resolve these issues through classical genetic screens and by exploiting new reverse genetic techniques to assay candidate genes identified by the essentially complete genome sequence of *C. elegans* (Consortium, 1998).

We show here that the intestine is a simple system for studying epithelial polarization in organogenesis. Intestinal organogenesis involves a small number of cells that form an epithelial tube with bilateral symmetry. We examine cytoskeletal changes associated with polarization of the intestinal primordium and show that microtubules play a role in that polarization. We further show that an isolated E blastomere is capable of generating a structure that has some, though not all, of the basic polarity characteristics of a normal intestine. Finally, we demonstrate that some of the events in the development of the intestine may be general features of epithelial morphogenesis in *C. elegans,* because similar events occur in the organogenesis of the pharynx.

MATERIALS AND METHODS

Nematode Strains and Culture

Wild-type (N2) *C. elegans* were cultured as described (Brenner, 1974). The JAM-1::GFP (*jcIs1*) strain contains a green fluorescent protein (GFP) marker for adherens junctions (Mohler *et al.*, 1998).

Light Microscopy

Our description of the development of the E descendants is based on 4D videomicroscopy of 15 living embryos, electron microscopic analysis of about 20 embryos, and immunohistochemical studies on between 10 and 50 embryos. Tubulin staining of embryos was performed as described by Costa *et al.* (1998). To visualize actin filaments, embryos were washed with dH_2O and attached to Teflon-coated slides (Erie Scientific) with 0.1% polylysine (Sigma). Embryos were permeabilized by gentle squashing under a glass coverslip and fixed for 10 min in 4% paraformaldehyde, 60 mM Pipes, 25 mM Hepes, 10 mM EGTA, 2 mM $MgCl_2$, 0.1 mg/ml L-α-lysolecithin (Sigma), pH 6.8. Fixed embryos were stained with BODIPY FL phallacidin (Molecular Probes) as described (Costa *et al.*, 1998). For immunostaining of embryos with mouse monoclonal ICB4 (Kemphues *et al.*, 1988), IFA (Pruss *et al.*, 1981), and MH27 (Francis and Waterston, 1991) antibodies and affinity-purified rabbit HMR-1 (Costa *et al.*, 1998), PKC-3 (Tabuse *et al.*, 1998), and ZYG-9 (Matthews *et al.*, 1998) antisera, embryos attached to polylysine-coated slides were permeabilized by freeze-cracking (Albertson, 1984). Embryos were fixed for 15 min in methanol at −20°C and washed twice with PBS-T (PBS + 0.1% Tween 20). Either PBS+1% BSA or PBS+10% normal goat serum was applied for 30 min before addition of primary antibodies. All primary antibody incubations were performed overnight at room temperature. The embryos were then rinsed twice with PBS-T and incubated with the appropriate FITC-, rhodamine-, or Cy-3-conjugated secondary antibodies. Before viewing, the embryos were rinsed twice with PBS. Nuclei were visualized by staining with 0.01 μg/ml DAPI (Sigma) or 0.2 μg/ml propidium iodide (Sigma) following RNase A treatment (0.2 mg/ml). Images of microtubules were acquired using a MRC600 confocal laser scanning microscope (Bio-Rad). All other images were acquired using a DeltaVision microscope and processed using deconvolution software (Applied Precision).

Four-dimensional Nomarski videomicroscopy was performed as described (Draper *et al.*, 1996). Lineaging and annotation of 4D movies were performed using Nematode Navigator V. B1 (kindly provided by Jason Pitt, http://www.fhcrc.org/science/basic/labs/priess/nn.html).

Electron Microscopy

Embryos were prepared for electron microscopy following the procedures of Priess and Hirsh (1986). Embryos at random stages of development were fixed together. These pooled embryos were examined under the dissecting microscope, and embryos at specific developmental stages were isolated and processed together.

Blastomere Culture

Culture and manipulation of isolated blastomeres was as previously described (Shelton and Bowerman, 1996), with the following modifications. Embryos and blastomeres were manipulated using drawn glass micropipettes of precise inner diameter. These micropipettes were attached to a mouth pipette for blastomere manipulations. Blastomeres were separated from each other by gently drawing in and blowing out cell aggregates with mouth pressure. A 45-μm micropipette was used to isolate EMS from late four-cell stage embryos. Following the division of EMS, a 40-μm micropipette was used to separate E from MS. Because E and MS are indistinguishable from each other at this stage, each was cultured in a separate drop of culture medium. Cultured blastomeres were kept in a humidity chamber between manipulations. After 8 h at 20°C, isolations were scored for nuclear position and birefringent gut granules.

Colcemid Treatment

Embryos were cut from gravid hermaphrodites and treated for 1 min in 1% NaOCl, 0.5 M KOH to aid in eggshell permeabilization. Embryos were then washed twice in M9 buffer (Brenner, 1974) and twice in embryonic culture medium (Shelton and Bowerman, 1996) with or without freshly added colcemid (Sigma) (stock solution 1 mg/ml in dH_2O) at a final concentration of 50 μg/ml. The eggshell was permeabilized at the anterior end of the embryo by laser irradiation until a pore large enough for the release of an embryonic cell was generated. In control experiments, release of an embryonic blastomere had no effect on cell polarization in the intestinal primordium.

Laser Cell Ablation

Laser ablations were performed as previously described (Mello *et al.*, 1992). For E isolations, the following cells were killed sequentially: AB, P2, and MS. Ablations were done before each division was complete so that both centrosomes and nuclei could be ablated. The ablated embryos were kept at room temperature for 5 h, at which point they were scored for nuclear position, birefringent intestinal granules, and lumen formation. For immunofluorescence, embryos were transferred to 0.1% polylysine-coated slides and processed as described above. For ablations at the E^4 stage, 20- to 50-cell embryos were isolated and prepared as described above. Embryos in a dorsal-up orientation were identified based on the position of the E^2 cells. Subsets of the E^4 primordium were killed by ablating the nuclei immediately following their birth. Embryos were scored 5 h after ablation for nuclear position and birefringent gut granules and processed for immunofluorescence.

RESULTS

The Digestive Tract

The *C. elegans* intestine consists of 20 cells that are derived clonally from a single embryonic precursor called the E blastomere. The cell division sequence of the E blastomere has been described previously by Sulston *et al.* (1983). We refer to the E descendants collectively as the intestinal primordium and indicate specific stages of the primordium as E^2, E^4, E^8, E^{16}, E^{18}, or E^{20} according to the number of E descendants present. We used 4D videorecordings to analyze the cellular events of intestine formation in living embryos. A schematic diagram of the major events and timing of intestinal development is shown in Fig. 1A.

The E blastomere is born on the surface of the embryo where it divides anterior/posterior. The E^2 cells migrate into the interior of the embryo at gastrulation, where they divide left/right; this is the only left/right division in the intestinal lineage. The E^4 and E^8 cells divide approximately anterior/posterior; however, some of these latter divisions are skewed toward the dorsal/ventral axis of the embryo. Thus the E^{16} primordium is a three-dimensional array of cells with a ventral tier of 6 cells and a dorsal tier of 10 cells; most of the E^{16} images presented in this paper are sections through the dorsalmost tier of cells. To facilitate reference to particular intestinal cells, we have assigned numbers to the E^{16} cells as indicated in Fig. 1A. The left/right pairs of No. 1 and 8 undergo an additional division to generate the E^{20} primordium; these divisions are dorsal/ventral and anterior/posterior, respectively. In most embryos, none of the E^{20} cells divide again, although they become binucleate and polyploid during postembryonic development (Hedgecock and White, 1985). We have occasionally observed one of the No. 5 cells divide during embryogenesis and presume this extra division is the basis for the 21 intestinal cells Sulston and Horvitz (1977) noted in a few newly hatched larvae.

We have used immunofluorescence (Fig. 2) and electron microscopy (Fig. 3) to study the cellular organization of the E^{20} intestine. We used an antiserum against the cadherin HMR-1 (Costa *et al.*, 1998) to stain adherens junctions (Fig. 2C) and the antibody ICB4 (Kemphues *et al.*, 1988) to stain intestinal cell surfaces (Fig. 2B). The basic anatomy of the E^{20} intestine can be represented as an anterior/posterior sequence of nine rings of cells (called int rings) that encircle the intestinal lumen (Figs. 1A and 2A; see also Sulston *et al.*, 1983). The int I ring consists of four symmetrical cells that originate from the dorsal/ventral division of the No. 1 E^{16} cells; all other int rings contain only two cells. On the basis of nuclear positions and cell boundaries, the int II, III, and IV rings appear to be rotated 90° relative to all other rings. Each intestinal cell has an apical surface that faces the central lumen and that is bordered by adherens junctions (see Fig. 1A for diagram). After immunostaining, the adherens junctions between cells in a given ring appear as longitudinal lines that run parallel to the long axis of the intestine; there are four such lines in int I and two in all other int rings (Fig. 2C). The adherens junctions between separate int rings appear as transverse and oblique lines, or simply as transverse lines, depending on whether cells in adjacent rings overlap (Fig. 2C, white arrowhead).

The ultrastructure of cells in the intestine is typical of intestinal cells in other animals, with each cell having distinct apical, lateral, and basal surfaces (Fig. 3). Adherens junctions appear as electron-dense foci at the borders of the apical (lumenal) membrane. The lumenal membrane consists of a microvillar brush border. The microvilli are coated

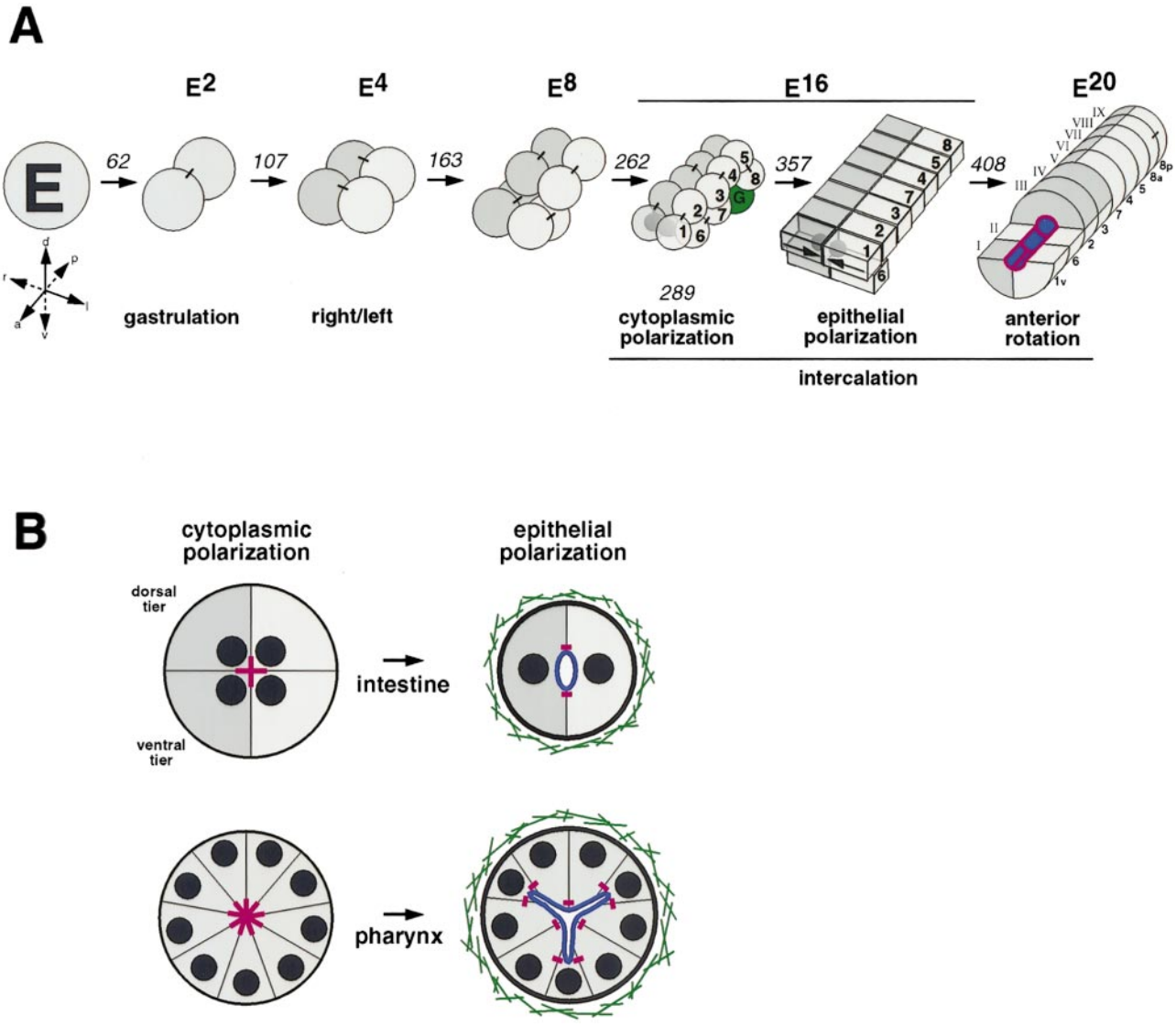

FIG. 1. Cellular events in organogenesis. (A) Schematic diagram showing the cell divisions and major events of intestinal organogenesis. Times are indicated in italics and represent minutes past the 2-cell stage of embryogenesis; on this scale the E blastomere is born at 35 min. For the E^{16} primordium, the anteriormost left/right pair of cells is shown transparent to indicate nuclear positions. The two germ cells (G) are on the ventral side of the E^{16} intestine, and one of these is shown in green. In comparison with the E lineage determined by Sulston *et al.* (1983), the E^{16} cells Nos. 1–8 are respectively Ealaa, Ealap, Eplaa, Eplap, Eplpa, Ealpa, Ealpp, and Eplpp. The intestinal rings (int rings) at the E^{20} stage are labeled with roman numerals following the convention of Sulston *et al.* (1983). The dorsal cells of the int I and II rings are removed to show the lumenal surface (blue) and the surrounding adherens junctions (magenta). The diagram is not to scale; the volume of the E blastomere is about the same as the volume of the entire intestine. (B) Schematic diagrams of cross sections through the intestinal and pharyngeal primordia. The cadherin HMR-1(magenta) is concentrated at the midline in the early primordia and later becomes incorporated into adherens junctions around the apical surfaces in the polarized epithelia. Basal surfaces (bold black lines) become associated with basement membranes (green) in the polarized epithelia.

with an electron-lucent matrix and are underlaid by a network of intermediate filaments, presumably equivalent to the glycocalyx and terminal web, respectively, of the vertebrate intestinal brush border. The basal membranes of the intestinal cells are covered by an extracellular basement membrane (Fig. 3).

As part of the present study, we compare some of the cellular events in the development of the intestine to the development of the pharynx. The embryonic origins of the cells in the pharynx have been determined (Sulston *et al.*, 1983), and the anatomy of the fully formed pharynx has been described (Albertson and Thomson, 1976). The phar-

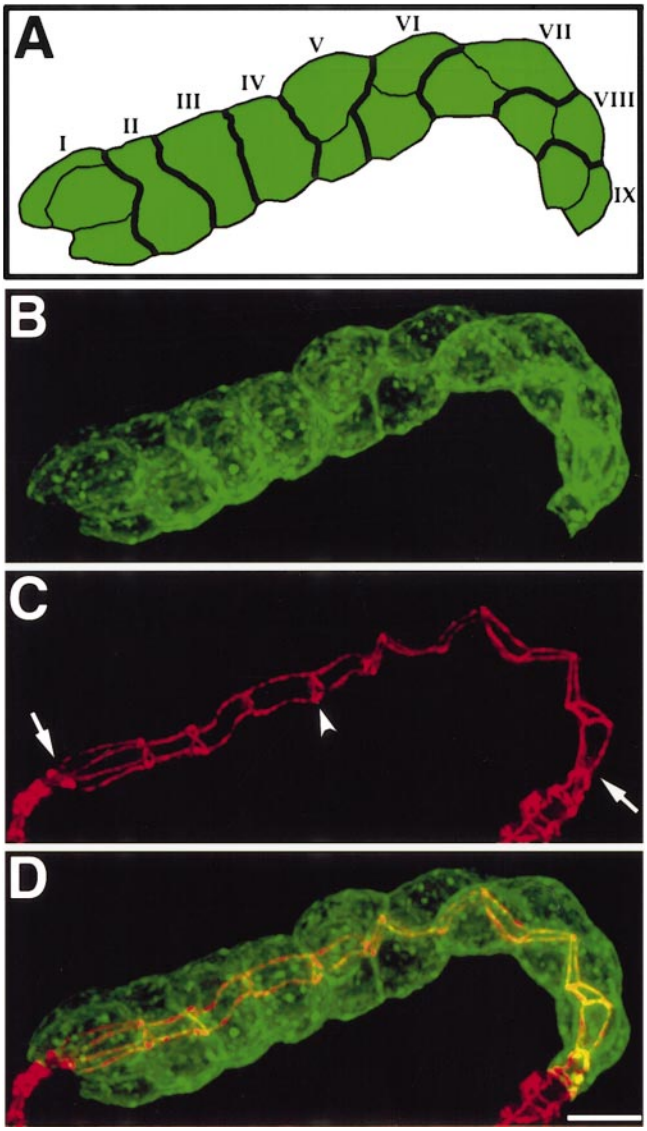

FIG. 2. Cytology of the E^{20} intestine. (A) Outline of the cells in an E^{20} intestine at about 500 min. Borders of the nine int rings are indicated in bold. Three of the four cells in int I are visible in this orientation. Only one of the two cells in each of the int II, III, and IV rings are visible because these rings are twisted counterclockwise 90° relative to the posterior rings (int V–IX). (B) Immunofluorescence image of an embryo stained with the antibody ICB4 to visualize intestinal cell membranes; A is drawn from this image. The small structure at the posterior (right) extreme of the intestine is the valve, which also stains with ICB4. (C) HMR-1 staining of the embryo in B showing adherens junctions in the intestine (region between the two arrows). See schematic diagram in Fig. 1A for relationship of adherens junctions to the intestinal lumen. (D) Combined images of B and C. Bar, 5 μm.

ynx, like the intestine, is essentially a monolayer of epithelial cells. The general structure of the pharynx resembles, in anterior to posterior sequence, a tube/cyst/tube/cyst, in which the terminal cyst is linked to the intestine by a set of valve cells. The pharynx has about four times the number of cells in the intestine and contains several cell types including neurons, glands, epithelial cells, and myoepithelial cells. Most of the cells have apical surfaces that border the Y-shaped, cuticle-lined lumen of the pharynx (see Fig. 7C). Our analysis will focus on the formation of these apical surfaces; other aspects of pharyngeal morphogenesis are being analyzed in detail by others and will be presented elsewhere (S. Mango, personal communication).

Cytoplasmic Polarization

By light microscopy, cells within the intestinal primordium first exhibit cytoplasmic polarization during the E^{16} stage (Fig. 4C). In previous stages each E descendant has a centrally located nucleus that is surrounded by yolk, lipid droplets, mitochondria, and Golgi (Figs. 4A and 4B, and data not shown). About 30 min into the E^{16} stage, nuclei of cells on the right-hand side of the intestinal primordium move to the left, and nuclei of cells on the left-hand side move to the right (Figs. 4C and 4D). These movements result in left/right pairs of nuclei clustered around an imaginary line running anterior/posterior through the center of the primordium. We will refer to this central line as the "midline" (M in all figures). At the time the E^{16} nuclei move toward the midline, cytoplasmic components move toward the opposite (future basal) surfaces (Figs. 4C–4F). The E^{16} cells elongate slightly along the left/right axis of the embryo, with a concomitant shortening of the primordium along the anterior/posterior axis.

Sections of the dorsalmost E^{16} primordium that are viewed by light (Fig. 5A) or electron microscopy (Fig. 6A) show the marked polarization of these cells. The nuclei become nearly juxtaposed to the cell membrane at the midline; this region becomes devoid of Golgi, yolk, and lipid droplets and contains only a few or no mitochondria (Figs. 5A and 6A). Vertical cross sections through the E^{16} primordium (Fig. 5B) show that both dorsal and ventral cells appear to be polarized toward the midline. Thus the primordium at this stage has radial symmetry with respect to the midline.

The pharyngeal primordium forms just anterior to the intestinal primordium (the outline of the pharynx is indicated by small black arrowheads in Fig. 4E and subsequent figures). Cytoplasmic polarization appears later in the pharyngeal primordium than in the intestinal primordium (Figs. 4G and 4H). In the light microscope, pharyngeal nuclei appear to move away from a central axis through the primordium (Fig. 4H); we call this central region the midline of the pharyngeal primordium. Cross sections through the pharyngeal primordium show that the cells become wedge-shaped, with their narrow tips extending toward the midline (Fig. 7A). Lipid droplets, yolk, mitochondria, and Golgi tend to accumulate between the cell nucleus and the midline of the primordium (Fig. 7A), though this stratification is less pronounced than in the polarized intestinal cells. Thus the intestinal and pharyngeal primordia both

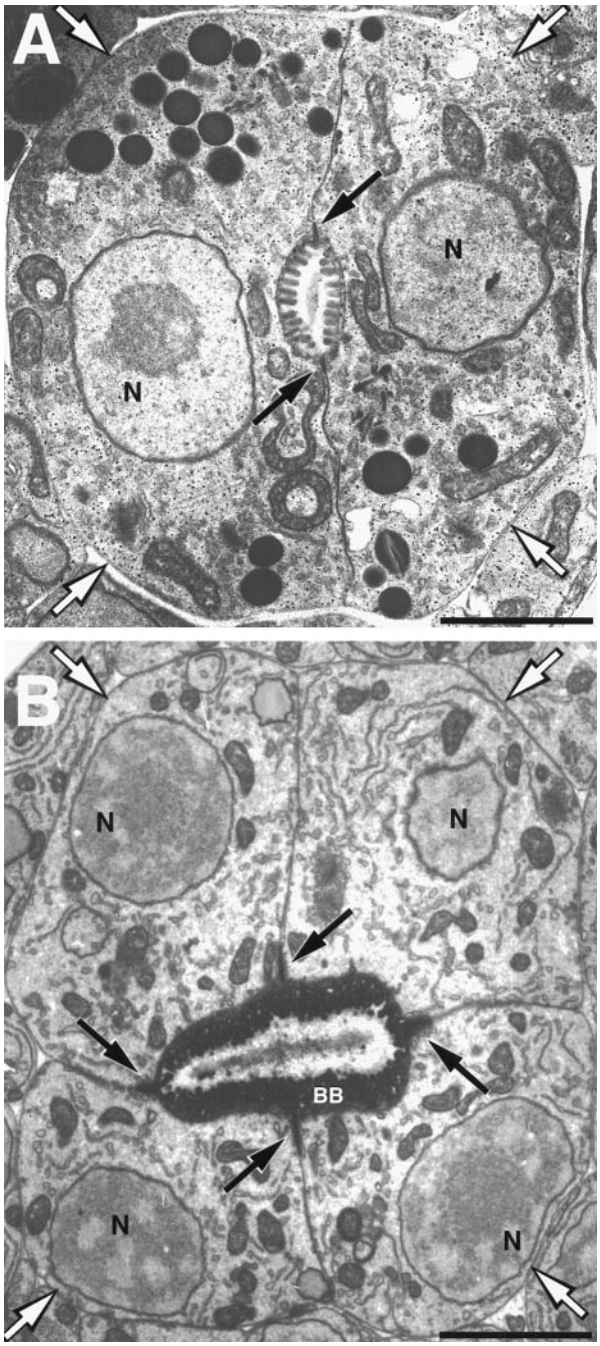

FIG. 3. Ultrastructure of the E^{20} intestine. Electron micrographs of cross sections through two int rings. (A) A posterior int ring in an embryo at about 600 min. (B) The int I ring in an embryo at about 800 min; this embryo is near hatching. Note that the brush border (BB) of the older embryo contains many more microvilli than in the embryo in A. The electron-lucent region around the microvilli in both images presumably is the glycocalyx. Black arrows point to adherens junctions surrounding the apical surfaces. A few intermediate filaments are visible underlying the brush border of the right cell in A; numerous intermediate filaments are associated with the microvilli in B, but are difficult to resolve at the magnification shown. White arrows point to the basement membrane surrounding the basal surfaces. Bars, 2 μm.

show radial symmetry with respect to the midline, although their nuclei move in opposite directions (see Fig. 1B for diagram).

Cell Separation at the Midline

Soon after cytoplasmic polarization, small and irregular gaps appear between cells at the midline in both the intestinal and the pharyngeal primordia (small black arrows in Figs. 4E and 4G). Sections through embryos at this stage confirm that the gaps correspond to cell separation at the midline (Figs. 5B and 5C). Though by light microscopy many of these gaps are transient, apparently collapsing or disappearing soon after they form, electron microscopy shows that small separations persist between cell membranes at the midline (data not shown). As described below, these midline regions eventually become the lumens of the intestine and pharynx.

Novel vesicles appear in the E^{16} intestinal primordium after cytoplasmic polarization is evident, but before membrane separation is detectable at the midline. The vesicles are enclosed by a membrane, are about 0.3–0.5 μm in diameter, and contain numerous internal granules or vesicles of about 0.05 μm (Figs. 6A and 6B). The vesicles are invariably localized at or near the midline, where they may be juxtaposed to the midline-facing membrane. These vesicles are the only cytoplasmic organelle found near the midline in the intestinal cells at this stage, except for occasional mitochondria and endoplasmic reticulum. Apparently identical vesicles are found near the midline in the pharyngeal primordium (Fig. 6C). In both the intestine and the pharynx, these vesicles appear continuously during lumen formation (see below) and remain concentrated near the lumenal surfaces of cells. Because the midline-facing cell surfaces correspond to the apical surfaces of the mature cells, we call these vesicles "apical vesicles."

A second, novel vesicle appears in the intestinal, but not pharyngeal, primordium after cytoplasmic polarization (these vesicles are labeled GG in Fig. 6A). These vesicles contain irregular patches of high electron density, and the vesicles localize to the basal region in cells along with most other cytoplasmic organelles. Based on the time these vesicles appear, their basal localization, and their occurrence in both larval and adult intestines (data not shown) we consider it very likely that these vesicles are the birefringent, autofluorescent, intestine-specific "gut granules" that are visible with polarization optics (see Fig. 13E) and that have been described previously (Cobb, 1914). Gut granules are thought to be involved in various aspects of catabolism (Babu, 1974; Clokey and Jacobson, 1986) and thus are unlikely to play any role in intestinal cell polarization.

Intercalation in the Intestinal Primordium

The bilateral symmetry of the intestine results from cell intercalation in the E^{16}–E^{20} primordium. A lateral view of the left side of the E^{16} primordium prior to intercalation is

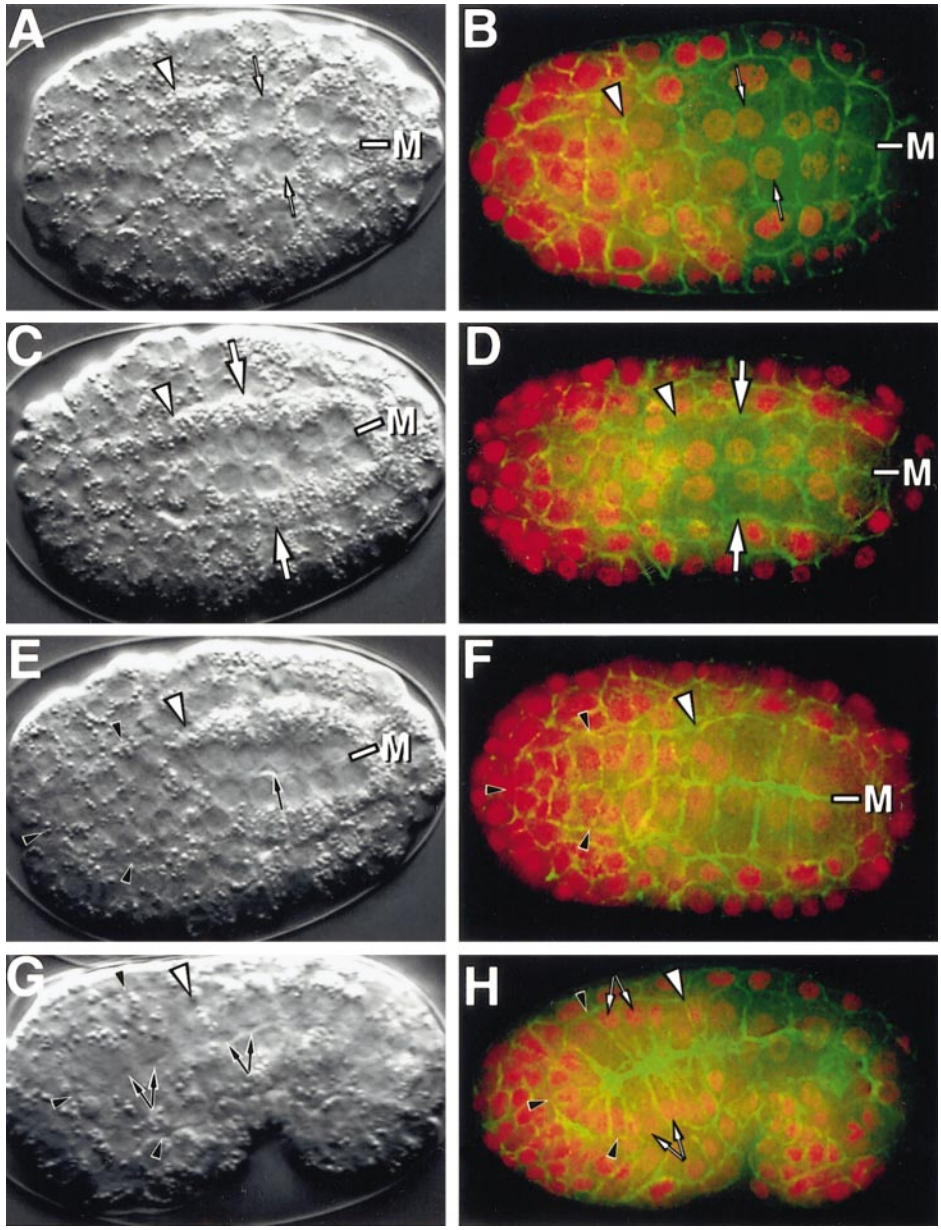

FIG. 4. Cytoplasmic polarization in the intestinal primordium. The left column shows a single live embryo at consecutive time points, and the right column shows fixed embryos at comparable stages stained for actin (green) and for DNA (red). Embryos shown are at (A and B) 265, (C and D) 290, (E and F) 315, and (G and H) 400 min. The intestinal primordium is at E^{16} in A–F, and at E^{18} in G and H. A–F show focal planes through the dorsalmost tier of E^{16} cells. In G and H, the embryo has rotated such that the images are lateral focal planes through the E^{18} primordium. The junction of the pharynx and intestine is indicated in all images by a white arrowhead, and the midline region is indicated by an M. During polarization the E^{16} nuclei move from central positions in the cells (small white arrows in A and B point to nuclei in the No. 3 cells) to midline positions (C and D), while cytoplasmic granules move to the periphery (arrows in C and D point to basal surfaces of the No. 2 cells). Cell separation at the midline is visible in E and G (black arrows). In E through H the outline of the pharyngeal primordium is indicated by black arrowheads. Note in H that the nuclei (small white arrows) in the pharyngeal primordium have moved basally, away from the midline. Embryos are about 50 μm in length; anterior is to the left.

shown in Fig. 8A and a schematic diagram of a similar stage is shown in Fig. 1A; five cells are on the dorsal tier (Nos. 1–5) and three cells are on the ventral tier (Nos. 6–8). We find that cells on the left side intercalate with other left cells in a stereotyped pattern (Fig. 1A), and cells on the right side intercalate with other right cells in the same pattern;

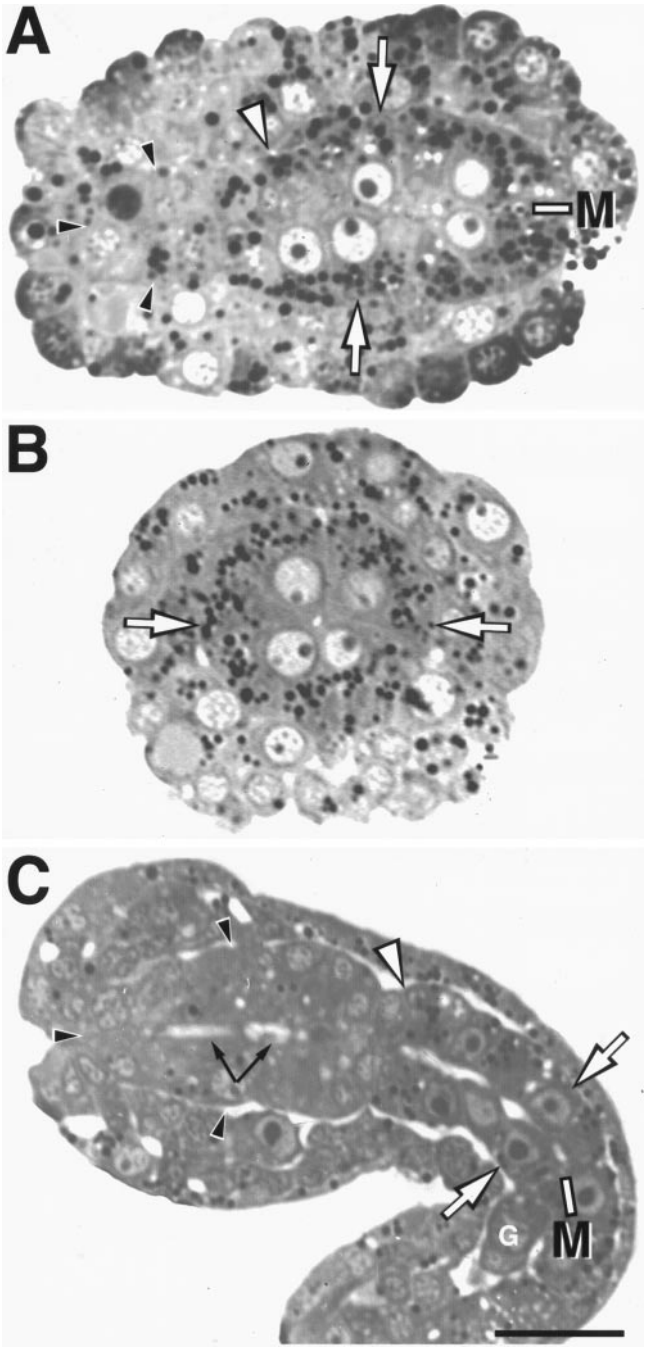

FIG. 5. Sections through the intestinal and pharyngeal primordia. Embryos fixed and embedded as for electron microscopy, but sectioned at 0.5 μm and photographed in the light microscope. (A and B) Embryos at about 330 min; the E^{16} primordium. A shows a dorsal section comparable to Fig. 4C, and B shows a cross section midway through the body. White arrows point to left and right intestinal cells. Five of the E^{16} nuclei are visible in A, and nucleoli are apparent in four of these. Yolk granules are localized to the outer, basal regions of the cells and appear here as small black dots; nuclei are localized toward the midline (M). Note the radial symmetry of the intestinal primordium in B; also note the separation of cell membranes at the midline (small white space at center; see also C). (C) Lateral section through an embryo at about 440 min. The intestinal primordium is at the E^{20} stage, and the body of the embryo has begun to elongate. Only the anterior half of the intestine is visible in this section; white arrows point to the right and left No. 3 cells (the int IV ring). Arrows and arrowheads are as described in Fig. 4. Bar, 10 μm; anterior is to the left in A and C.

we have never observed left or right cells intercalate across the midline. Two distinct intercalation events occur, one in the E^{16} primordium involving the No. cells 7 (see Fig. 8C) and another in the E^{20} primordium involving the No. 6 cells (see Fig. 9). After intercalation, all of the left cells have a polarity that is opposite that of the right cells. Thus the intestinal primordium changes from having radial symmetry in cross section to having bilateral symmetry (Fig. 1B). As the No. 6 cells intercalate, neighboring cells begin a coordinated, circumferential migration around the axis of the midline. These are the Nos. 6 (int II), 2 (int III), and 3 cells (int IV). These movements result in the "rotated" appearance of the int II, III, and IV rings characteristic of the fully formed intestine (Figs. 1, 2, and 8D; see also Sulston *et al.*, 1983). In subsequent development the entire intestinal primordium elongates along the anterior/posterior axis of the embryo. We have not examined the basis for intestinal elongation in detail. However, its elongation is likely to depend on the elongation of the embryo; experimental conditions and mutant backgrounds that prevent body elongation also prevent intestinal elongation (our unpublished results and Priess and Hirsh, 1986).

Cross sections of the intestine prior to intercalation show the midline zone of cell separation between four, radially symmetrical cells (Figs. 1B and 5B). However the lumen of the fully differentiated intestine is bordered, in general, by only two cells (Figs. 1B and 3A). Do cells define a new lumenal site after they intercalate that is distinct from the early zone of cell separation? To address this issue we made 4D videorecordings of lateral views of embryos during intercalation, such that the zone of cell separation and the intestinal cell membranes could be monitored simultaneously. We found that the zone of cell separation remained fairly constant in position during intercalation, with the intercalating cells extending processes around this zone (Fig. 9); the zone of cell separation in the primordium coincided with the position of the intestinal lumen.

Formation of the Apical Surface/Epithelial Polarization

Adherens junctions are present near the junction between the apical and the lateral surfaces of all epithelial cells in *C. elegans*, and their formation is considered a hallmark of epithelial polarization (White, 1988). The adherens junctions contain actin (Fig. 4H), the cadherin HMR-1 (Fig. 2C), and an antigen recognized by the antibody MH27 (Fig. 10A) that has not yet been described molecularly, but is not

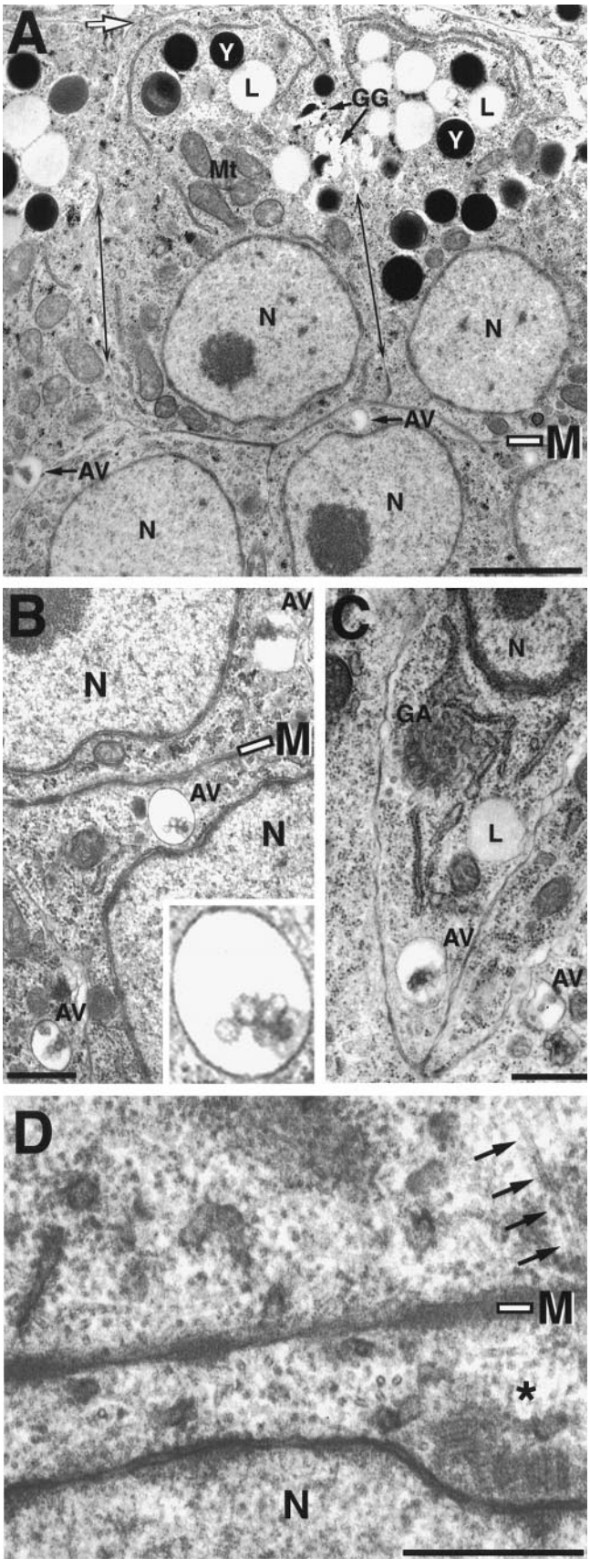

HMR-1 (Priess and Hirsh, 1986; Francis and Waterston, 1991; Costa *et al.*, 1998). Prior to the E^{16} stage, HMR-1 is detectable at low levels on or near the membranes of all cells in the embryo (Costa *et al.*, 1998). In the E^{16} intestinal primordium, HMR-1 and the MH27 antigen accumulate to very high levels near the midline (Figs. 8A and 8B, and data not shown). A gap in the immunostaining pattern at the midline is observed reproducibly between a pair of left/right cells (No. 4 in Figs. 1A and 8B). These cells are in the dorsal tier of the E^{16} primordium and are the only dorsal cells that do not contact intestinal cells in the ventral tier; the ventral positions are occupied by the germ cell precursors (labeled G in Fig. 8A). As the No. 7 cells in the intestinal primordium intercalate, we detect actin (Fig. 4F), HMR-1, and the MH27 antigen (data not shown) at the cellular interface between all left/right pairs of cells. Following cell intercalation, the initially punctate staining patterns merge into the rectilinear pattern characteristic of the adherens junctions surrounding the lumen of the mature intestine (Figs. 2C and 8C). In the pharyngeal primordium, HMR-1 and the MH27 antigen also appear as punctate foci along all nonbasal membranes (data not shown), and then become localized to the midline in a rectilinear pattern (Figs. 8C and 10A).

An antiserum against PKC-3, a *C. elegans* protein related to mammalian atypical protein kinase C, provides a marker for early apical differentiation in the intestinal and pharyngeal primordia. This antiserum has been reported previously to stain the intestinal lumen in *C. elegans* (Wu *et al.*, 1998). We find that this antiserum shows a pattern of immunostaining in embryos at about 300 min that closely resembles the staining patterns of adherens junctions components such as HMR-1 (Fig. 8A and data not shown). However, by 420 min PKC-3 staining is distinguishable from the HMR-1 pattern; PKC-3 staining is restricted to the apical surface membrane within the adherens junctions

FIG. 6. Ultrastructure of cells after cytoplasmic polarization. Electron micrographs of cells in the primordia of the intestine (A, B, and D) and pharynx (C). Structures indicated are the midline (M), nuclei (N), lipid droplets (L), yolk granules (Y), gut granules (GG), mitochondria (Mt), the Golgi apparatus (GA), and apical vesicles (AV). (A) Electron micrograph of the dorsal tier of E^{16} cells (about 330 min) near the midline, section level similar to Fig. 5A. The lateral (double-headed arrows) and basal (white arrow) membranes of one E^{16} cell are indicated. Bar, 2 μm. (B) Apical vesicles at the midline. Note internal granules in all apical vesicles. Bar, 0.5 μm. Inset shows a 3× magnification of a single apical vesicle. (C) Wedge-shaped cells in the anterior of the pharyngeal primordium at about 400 min. Apical vesicles are visible near the tips of the cells. Bar, 0.5 μm. (D) High magnification of region near the midline of the intestinal primordium at about 330 min. Several microtubules are visible near the midline (arrows point to one orthogonal microtubule in the upper cell). The nucleus of the lower cell has centrioles (below the asterisk) on its midline-facing surface. Bar, 0.05 μm.

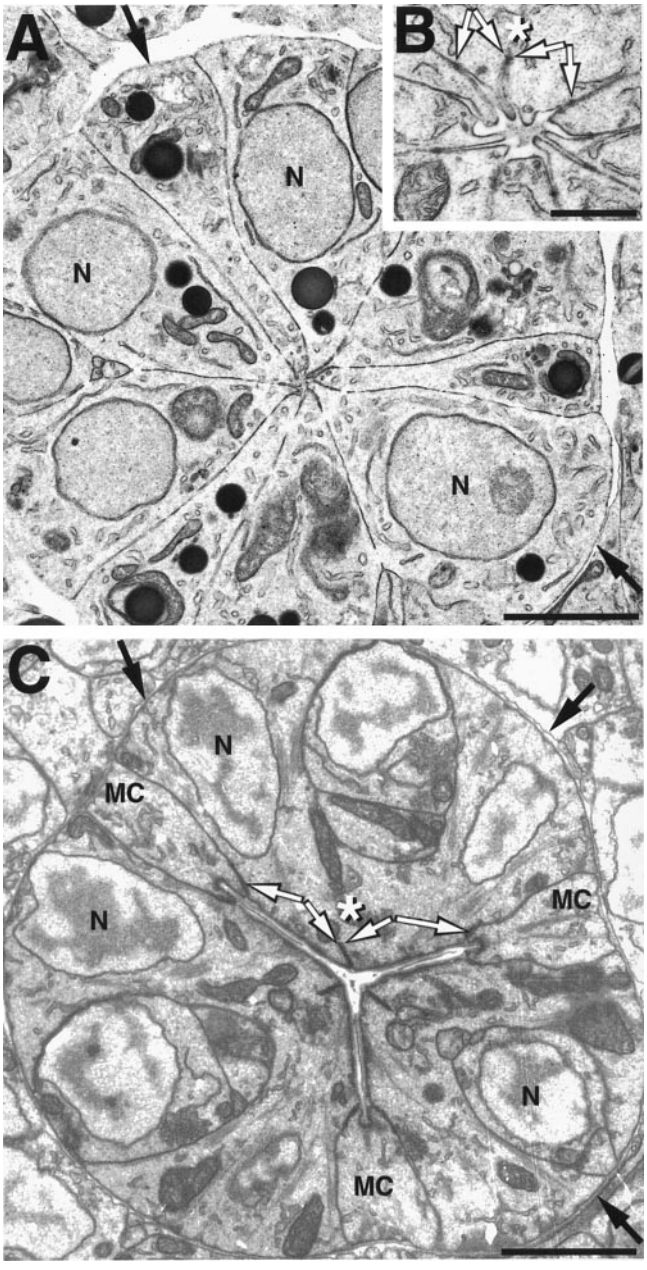

FIG. 7. Ultrastructure of the pharyngeal primordium after polarization. Electron micrographs of cross sections through the pharynx; black arrows point to the basal surfaces of pharyngeal cells (compare with Fig. 1B). (A) Embryo at about 400 min. Nine cells have become wedge-shaped with narrow tips at the midline (center). Bar, 2 μm. (B) High magnification of the midline region in the pharyngeal primordium of an embryo approximately 30 min older than the embryo shown in A. The zone of cell separation is evident at the midline, and electron-dense adherens junctions are visible between the tips of each of the nine cells. The double arrows on each side of the asterisk point to the adherens junctions in the tip of one cell. Bar, 0.5 μm. (C) Formation of the Y-shaped lumen in late embryogenesis. As in (B), the double arrows on each side of the asterisk point to adherens junctions. Note that the positions of the outside arrows have changed considerably because the three marginal cells (MC) have retracted their tips from the midline. Nuclei (N) have differentiated and become heterochromatic. The basement membrane surrounding the pharynx is visible beneath the black arrow at the top right, and intermediate filaments are visible in the marginal cell on the right. Bar, 2 μm.

(Fig. 10). A similar, apically restricted staining pattern of PKC-3 is observed in the pharyngeal primordium (Fig. 10)

In electron micrographs of the intestinal and pharyngeal primordia, adherens junctions are observed to form very close to the zone of cell separation. In cross sections of the pharyngeal primordium, electron-dense adherens junctions appear between the tips of each of the wedge-shaped cells (Fig. 7B). During subsequent embryogenesis, the apical surface area of the pharynx expands as three of these cells retract their tips from the midline, forming the Y-shaped lumen characteristic of the *C. elegans* pharynx (Fig. 7C). The three retracting cells are unique in developing intermediate filaments that run between their apical and basal surfaces (Fig. 7C), and these cells are thus identifiable as the marginal cells of the pharynx as described by Albertson and Thomson (1976). The apical surface of the intestine also expands during subsequent embryogenesis. Though in cross sections of the intestine, the linear distance between the adherens junctions appears to be fairly constant, the apical membrane between the adherens junctions increases in area as numerous microvilli develop (Figs. 3A and 3B).

As the apical surfaces of the intestinal cells and pharyngeal cells differentiate, electron micrographs show basement membranes developing on the basal surfaces of these cells (Figs. 3A and 7A). The marked cytoplasmic polarization evident in the earlier primordia gradually diminishes or disappears; intestinal nuclei are found in the center of the cytoplasm, and cytoplasmic granules appear to be distributed randomly throughout the cell (Figs. 3A).

Cytoskeletal Basis for Early Polarization

In several electron micrographs of the E^{16} primordium after cytoplasmic polarization, we observed centrosomes associated with some nuclei. These centrosomes were usually on the surface of the nucleus facing the midline (Fig. 6D). This observation indicated that at least some centrosomes must become repositioned after the E^{8} to E^{16} cell division, because this division is along the anterior/posterior axis of the primordium (see Fig. 1A). In addition, we noticed there were two centrosomes (each containing two centrioles) associated with some of the E^{16} nuclei, suggesting that the cells had duplicated their centrosomes (data not shown). This result was surprising because 12 of the E^{16} cells do not undergo subsequent cytokinesis, and centrosome duplication is not a common feature of postmitotic cells.

For a detailed analysis of centrosome behavior in the intestinal primordium, we stained embryos with the anti-

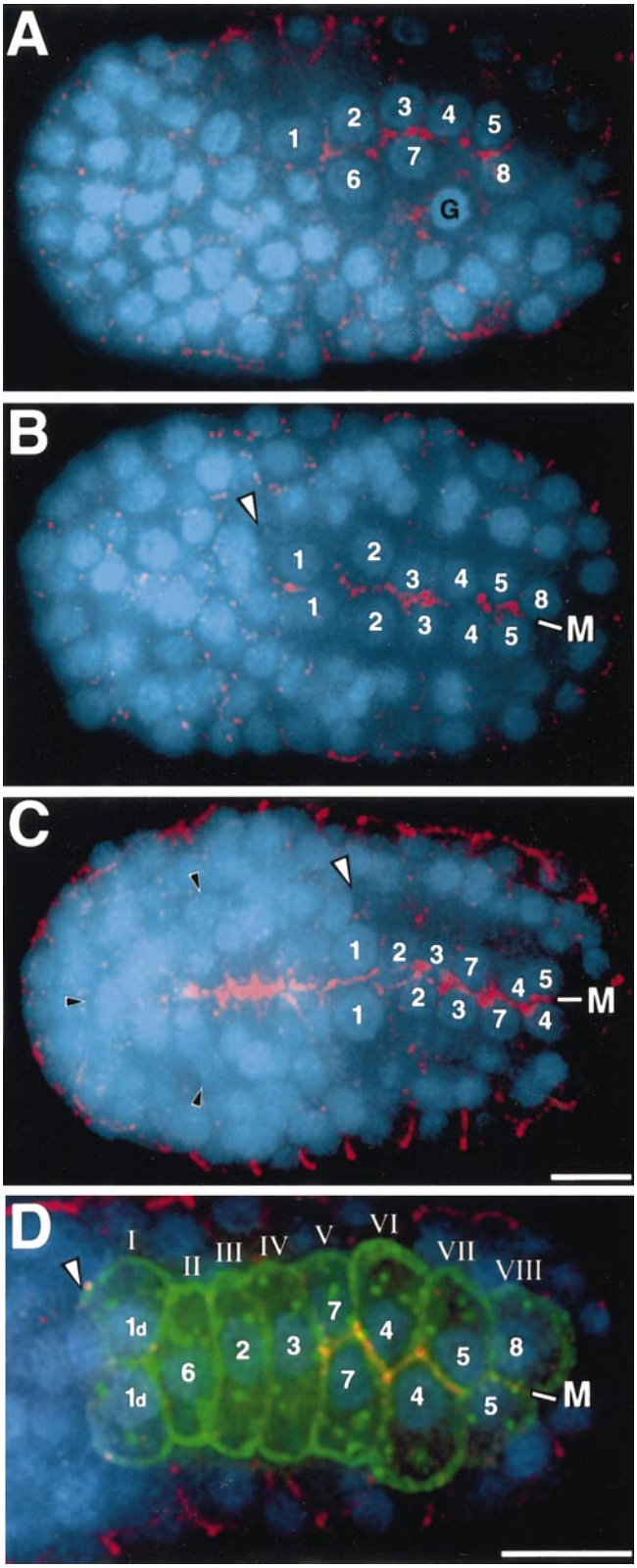

FIG. 8. Formation of adherens junctions and rotation of the anterior int rings. Immunofluorescence micrographs of embryos stained for the HMR-1 cadherin (red) and for DNA (blue). (A) Lateral focal plane of embryo at about 300 min showing the left half of the E^{16} primordium; compare with diagram in Fig. 1A. Five intestinal cells are in the dorsal tier (nuclei 1–5) and three are in the ventral tier (nuclei 6–8). Note that cell 4 sits over the germ cell precursor (G) rather than over another intestinal cell. (B) Dorsal focal plane of embryo at the same age as in A, showing the dorsalmost tier of E^{16} cells. Note the lack of HMR-1 staining between the left and right No. 4 cells. (C) Dorsal focal plane of embryo at about 350 min showing the dorsalmost nuclei in the E^{16} primordium. Nuclei in the No. 1 cells (under white arrowhead) have enlarged and are about to divide. HMR-1 is beginning to localize into the rectangular shapes characteristic of adherens junctions in the mature intestinal cells (compare to Fig. 2C). The No. 7 nuclei have intercalated between the No. 3 and 4 nuclei. Note that HMR-1 has become concentrated at the midline in the pharyngeal primordium (outlined by black arrowheads). (D) High magnification of a dorsal section through the E^{18} primordium at about 375 min. Intestinal cell membranes (green) have been stained with the antibody ICB4. Note that cells in the int II, III, and IV rings have rotated 90° with respect to surrounding cells, so that only one nucleus is visible; compare with Fig. 2A. Bars in C and D, 5 μm.

body IFA (Pruss *et al.*, 1981). This antibody was raised against a mammalian intermediate filament protein, and was subsequently shown to stain intermediate filaments in late-stage *C. elegans* embryos (Priess *et al.*, 1987; Francis and Waterston, 1991). In addition to this staining pattern in late embryos, we discovered that early *C. elegans* embryos had a punctate staining pattern throughout the cell cycle that was suggestive of centrosomes. For example, there was one dot of IFA staining in the center of each mitotic spindle aster (Fig. 11A) that became two dots following mitosis. An antiserum against the ZYG-9 protein has been shown to stain a mitosis-specific "halo" around centrosomes in *C. elegans* (Matthews *et al.*, 1998) and we found that the dots stained by IFA were localized within the ZYG-9 halo (Fig. 11). We therefore believe the structures recognized by IFA are very closely associated with centrosomes and will refer to these structures as centrosomes in the following description.

Immunostaining with IFA shows that after the E^{8} division, each E^{16} cell inherits one centrosome; this centrosome is located in the anterior or posterior region of the cell, as expected from the orientation of the E^{8} mitotic spindle (double-headed arrows in Fig. 12A). Consistent with our electron microscopic studies, we found that the centrosomes in each E^{16} cell duplicated into two separate centrosomes within about 10 min (Fig. 12A, asterisk). The duplicated centrosomes appeared to rotate toward the midline (Fig. 12B); for example during cytoplasmic polarization about 80% (n = 150) of the E^{16} cells had both centrosomes facing the midline. In contrast, centrosomes did not appear to face the midline in the pharyngeal primordium (data not shown).

Centrosome rotations have been described in the early blastomeres of the *C. elegans* embryo and shown to require microtubule function (Hyman and White, 1987). We there-

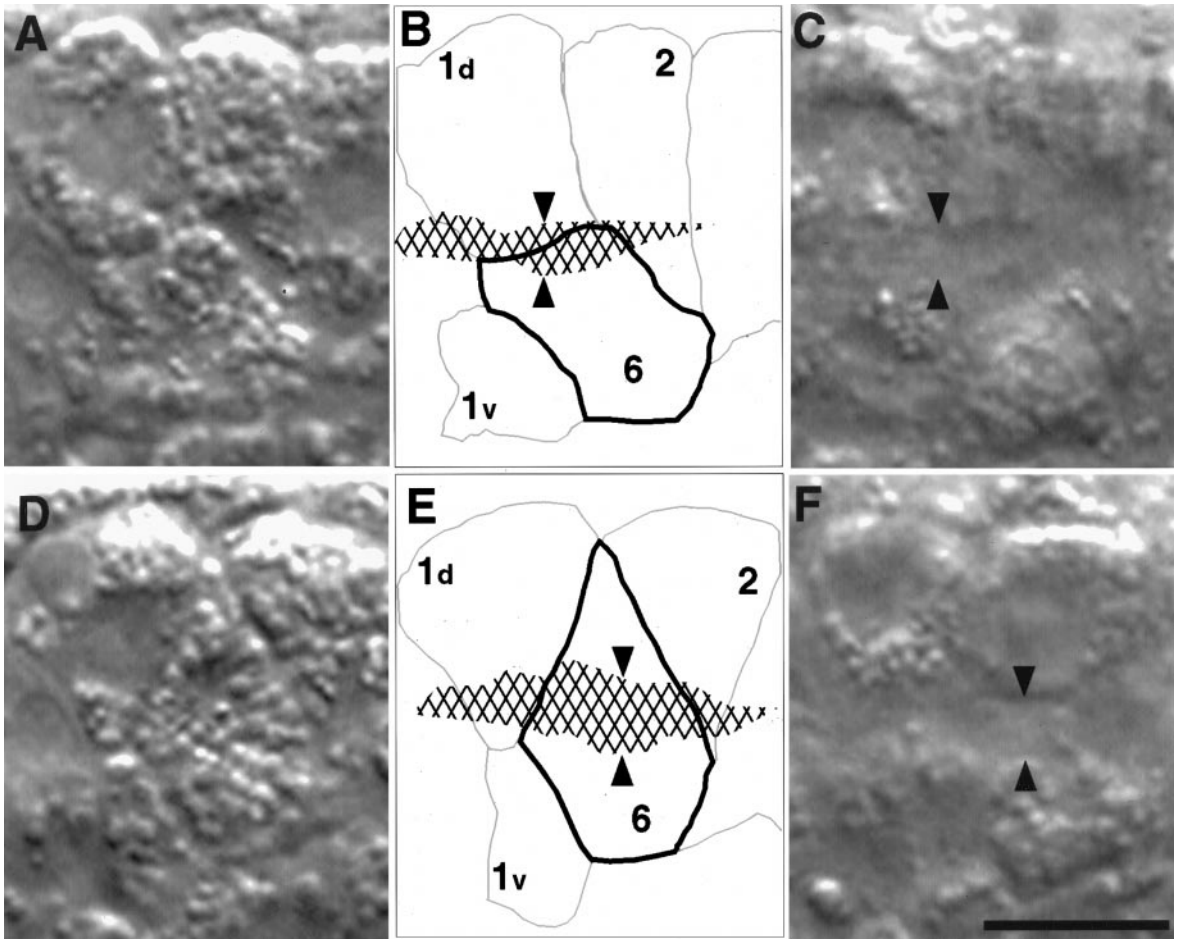

FIG. 9. Cell intercalation across the zone of cell separation. The top row (A–C) shows two different focal planes of anterior cells on the right lateral side of the E^{20} primordium. The embryo shown is about 400 min. A shows the outer surface membranes, and C shows the inner surface where the midline zone of cell separation is indicated by arrowheads. (B) Composite diagram of intestinal cells (outline) and zone of cell separation (hatching). Embryo stage and orientation is similar to that of Fig. 4G. The bottom row (D–F) shows corresponding images of the same embryo 15 min later. Note that cell No. 6 has begun to intercalate and has extended a process around the zone of cell separation. Bar, 5 μm.

fore examined microtubules in E^8 and E^{16} cells by immunostaining and by electron microscopy. Microtubules appear to associate uniformly with the surfaces of E^8 cells and with other embryonic cells (data not shown). In contrast, E^{16} cells had a highly asymmetric distribution of microtubules (Fig. 12C). Microtubules were concentrated near the midline, where they appeared to emerge in a fountain-like array and extend along the lateral surfaces of the cells. By confocal microscopy, relatively few microtubules were visible along the basal surfaces. Numerous microtubules were in the vicinity of the centrosomes (Figs. 6D and 12C). Because of the concentration of microtubules at the midline, we think it is likely that there is a microtubule organizing center at the midline; however, we could not determine by these studies whether any microtubules were emanating from the centrosomes. After intercalation of the No. 7 cells in the primordium, microtubules remained concentrated at the interface between contralateral cells (data not shown). Centrosomes appeared to be oriented more randomly at this later stage. For example, about 47% (n = 184) of the late E^{16} cells had one or both centrosomes on the basal-facing surface of the nucleus.

To examine whether microtubules were required for cytoplasmic polarization, we permeabilized embryos in culture media with or without the microtubule inhibitor colcemid immediately after the birth of the E^{16} cells (Fig. 13). In embryos that were not exposed to colcemid, the E^{16} cells showed cytoplasmic polarization and nuclear localization to the midline within 30 min (n = 7; images taken at 75 min for Figs. 13C and 13E), similar to the normal timing of polarization. In embryos exposed to colcemid, the E^{16} cells showed no evidence of cytoplasmic polarization within 75 min (n = 8; Figs. 13D and 13F). During this interval, nuclei stayed at a central position in the cell, and cytoplasmic

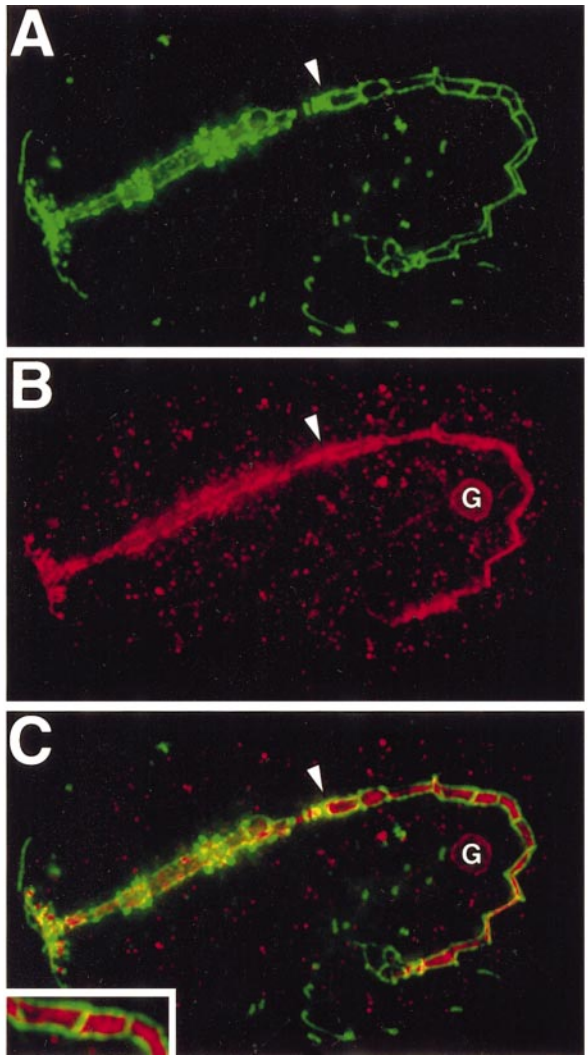

10

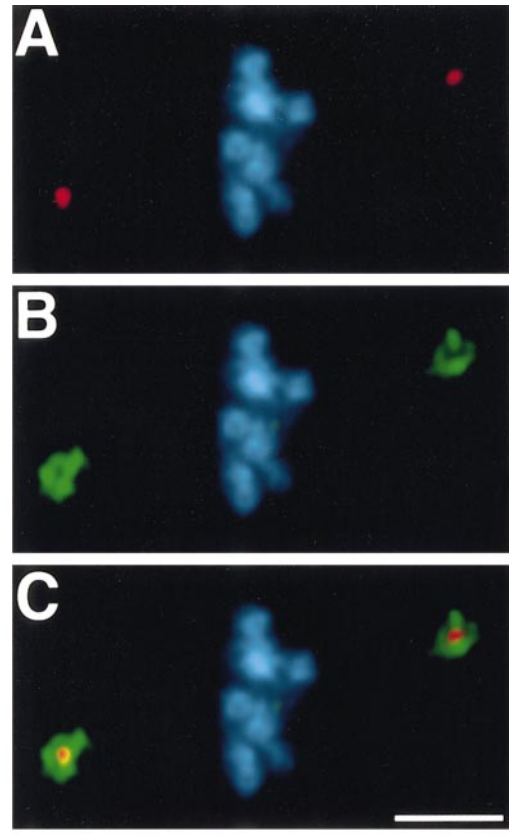

11

FIG. 10. PKC-3 is an early marker for the apical surface. Immunofluorescence images of a single embryo at about 420 min; compare with Fig. 5C. The embryo has been stained for (A) the adherens junction marker MH27 and (B) for PKC-3. The intestine lies to the right of the white arrowhead, and the pharynx is on the left. (B) PKC-3 staining is prominent throughout the midline of the pharynx and intestine and in the germ cell precursor (G) below the intestine. (C) Merged image from A and B. The inset shows the region of the intestine above the germ cell at higher magnification. Note that the PKC-3 staining is bordered by adherens junctions and so corresponds to the apical surface of the intestine.

FIG. 11. IFA stains centrosomes in *C. elegans*. High magnification of the spindle region of a one-cell-stage embryo after immunostaining with (A) IFA and (B) anti-ZYG-9 antiserum. The metaphase chromosomes are stained by DAPI (blue, all images). (C) Merged image from A and B. Bar, 2.5 μm.

components that normally become basal (gut granules, yolk, lipid) remained dispersed throughout the cytoplasm. However, with subsequent incubation many of the E^{16} cells became at least partially polarized in seven of the eight experimental embryos. We fixed and stained two of these embryos for tubulin and could not detect microtubules. Thus this late polarization either was independent of microtubules or involved a small number of microtubules that could not be detected by immunostaining. We conclude that microtubules are required for the rapid cytoplasmic polarization observed in normal E^{16} cells, though other mechanisms may also contribute to the polarized state.

Autonomy of Intestinal Organogenesis

E blastomeres that are isolated from all other blastomeres have been shown to produce descendants with at least some intestine-specific gene expression (Laufer *et al.*, 1980; Schroeder and McGhee, 1998). We wanted to examine whether these descendants had any ability to undergo

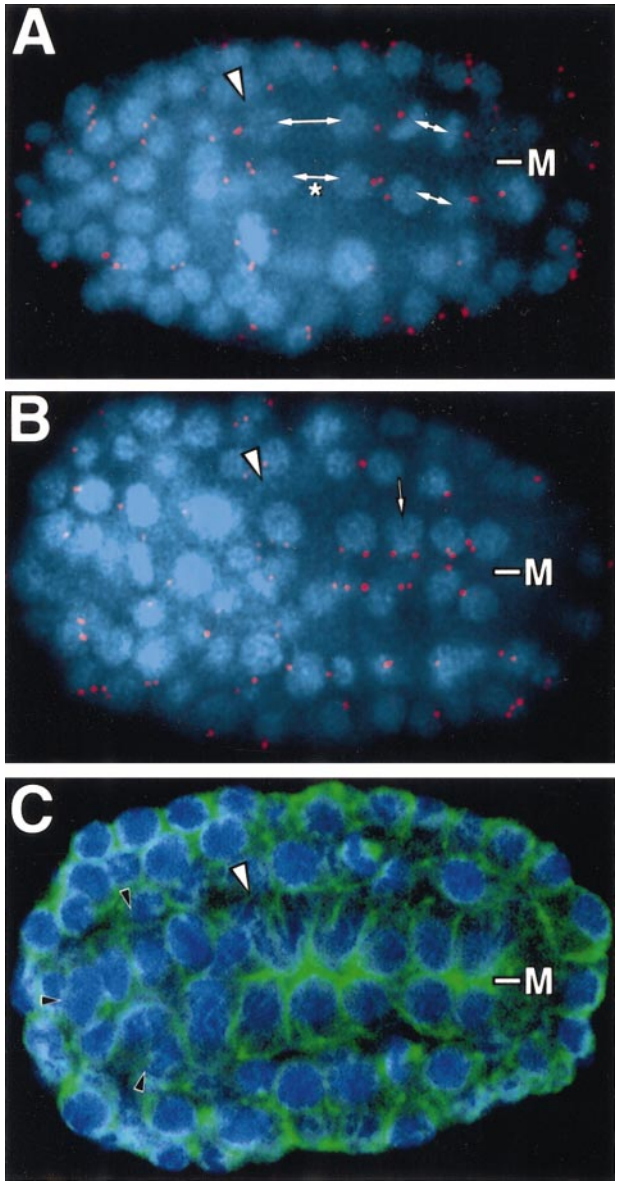

FIG. 12. Centrosomes and microtubules in the intestinal primordium. (A and B) Immunofluorescence micrographs of embryos stained with IFA to visualize centrosomes (red) and with DAPI to visualize nuclei (blue). All images are dorsal focal planes through the dorsalmost tier of the intestinal primordium. (A) Embryo at about 255 min during the division of E^8 to E^{16}. Sister nuclei are indicated by double-headed arrows. Note that the sister cells above the asterisk have already duplicated their centrosomes. (B) Embryo shown is slightly older than in A. The centrosomes have duplicated and become positioned near the midline. (C) Immunofluorescence micrograph of embryo at E^{16} stained for tubulin (green) and for nuclei (blue). Embryo is about the same age as in B. Note concentration of microtubules near the midline (M).

morphogenesis. In one set of experiments, we physically isolated E from other blastomeres and allowed it to divide in culture medium (Figs. 14A and 14B). In the second set, we used a laser microbeam to ablate all of the embryonic cells except the E blastomere (Fig. 14C). In both sets of experiments, E produced 16–20 cells that formed a cyst-like structure around a central, extracellular cavity (n = 4/4 and 9/9, respectively; black arrows in Figs. 14A–14C). All E descendants differentiated intestine-specific granules (data not shown) and appeared to have a common polarity with respect to the central cavity of the cyst; the nuclei were localized asymmetrically toward the cavity, and gut granules, yolk, and lipid droplets were concentrated at the opposite pole. Adherens junctions formed at the cell surfaces facing the cavity (Figs. 14G and 14J), and the apical marker PKC-3 appeared to localize within the borders of the adherens junctions (Figs. 14K and 14L). Thus, the cells become apically polarized toward a central cavity or lumen, as in the normal intestinal primordium. However, they do not form bilaterally symmetrical tubes resembling the normal intestine.

In the normal intestine, all cells that originate from the left side of the primordium eventually have a cytoplasmic polarity that is opposite to that of cells from the right. We

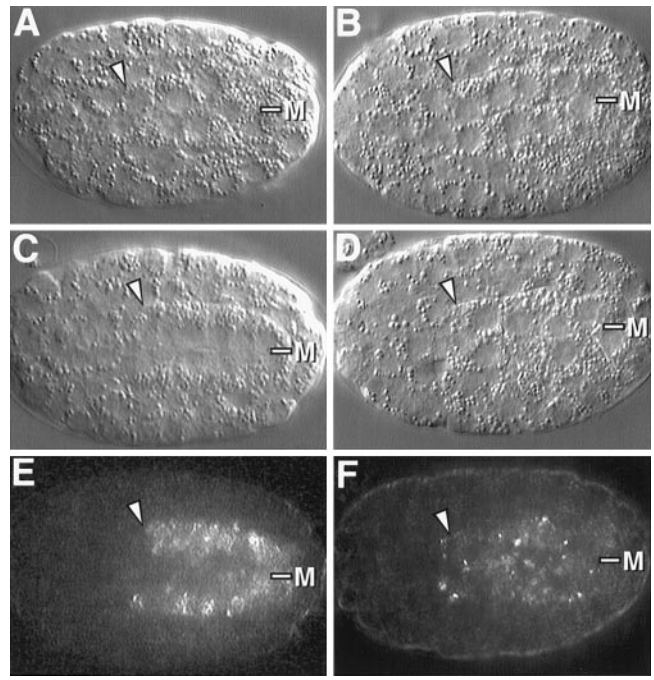

FIG. 13. Microtubules function in cytoplasmic polarization. The left column (A, C, and E) shows a single permeabilized embryo in culture medium without colcemid, and the right column (B, D, and F) shows a single permeabilized embryo of the same age in culture medium containing colcemid. Embryos were permeabilized immediately after the E^8 to E^{16} division. (A and B) Embryos 5 min after permeabilization. (C and D) Embryos 75 min later. Embryos in C and D viewed with polarization optics. Intestine-specific "gut granules" are birefringent and appear as small white dots. Cytoplasmic polarization is evident only in the embryo that was not exposed to colcemid.

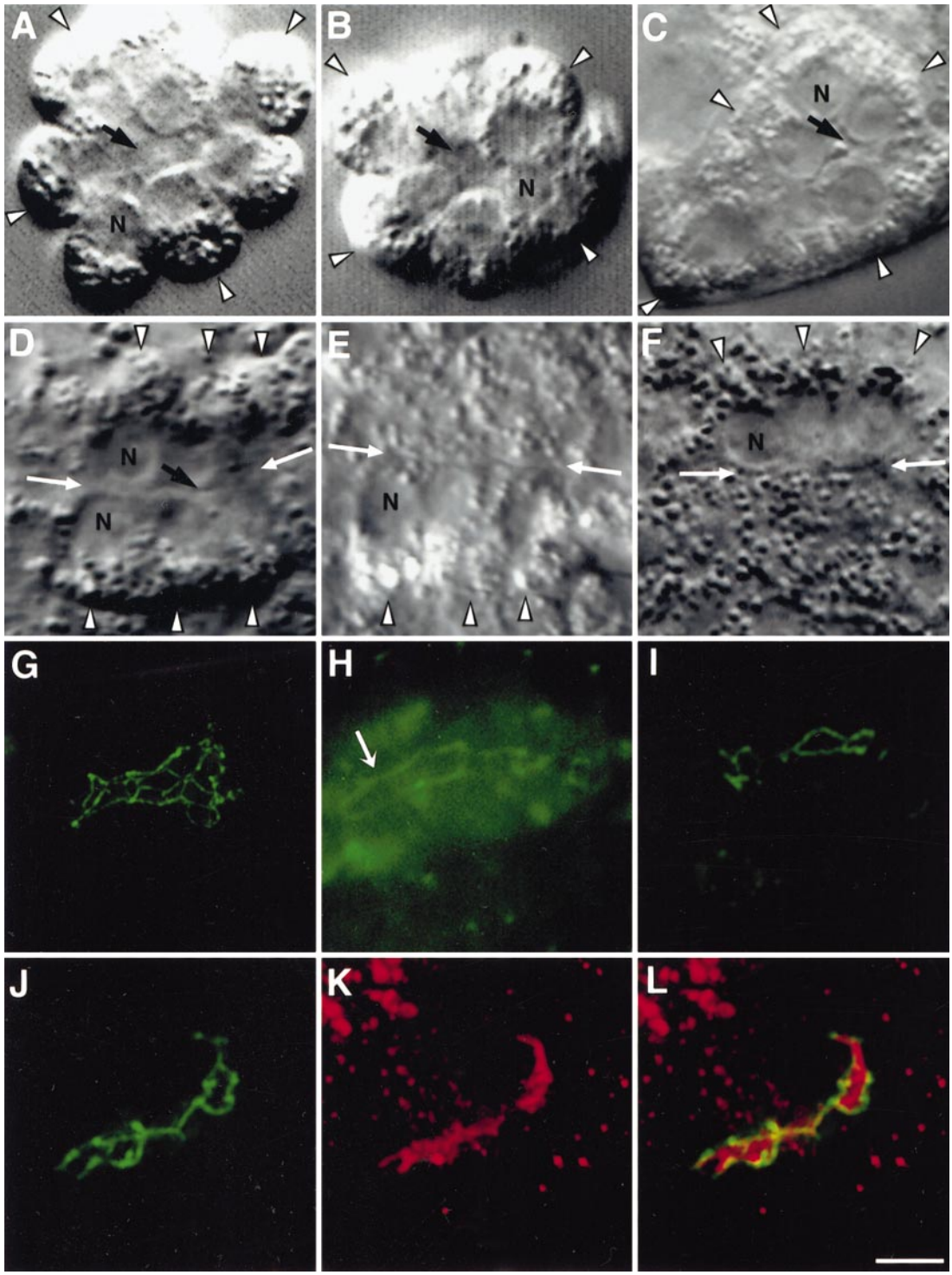

FIG. 14. Cell autonomy in intestinal organogenesis. (A–C). Focal planes through the centers of the cysts formed from isolated E blastomeres grown in culture (A and B) or after all other blastomeres were killed (C). White arrowheads point to the basal surfaces of cells, and the black arrows point to cavities at the center of each cyst. Note that the nuclei are asymmetrically positioned proximal to the cavities, while cytoplasmic granules are positioned distally. (D–F) Partial intestines formed after ablation of subsets of the E^4 primordium. White arrowheads and black arrows are as in A–C. White arrows indicate the center of the embryo, corresponding to the normal location of the midline. (D) Half-intestine derived from the anterior left/right pair of E^4 cells. (E) Half-intestine derived from the left pair of E^4 cells. (F) Half-intestine derived from the right pair of E^4 cells. (G) Adherens junctions in a cyst such as in C after staining with MH27; note the

therefore used 4D time-lapse recordings to follow the development of an isolated E after killing all other cells to see whether left/right origins were correlated with subsequent polarity. This was not the case; in several examples adjacent cells had the same polarity irrespective of their left or right origins (data not shown). These results suggest that E descendants have an intrinsic ability to polarize coordinately in the same direction, forming cysts with radial symmetry. The bilateral symmetry of the normal intestine must therefore depend upon additional contributions from nonintestinal cells.

To examine how left/right differences, and thus bilateral symmetry, are established in the normal primordium, we used a laser beam to kill specific pairs of cells in the E^4 primordium in an otherwise intact embryo. In the E^4 primordium there is an anterior pair of left/right cells and a posterior pair of left/right cells (Fig. 1A). We found that the anterior left/right pair could form a relatively normal, half-intestine with bilateral symmetry after the posterior left/right pair was killed (n = 12/12; Fig. 14D). In these experiments, nuclei were localized at the midline, cytoplasmic granules were localized to the opposite pole, membrane separation occurred at the midline (black arrow in Fig. 14D), and adherens junctions formed in a rectilinear pattern between left/right cells (Fig. 14H). We obtained identical results from the posterior left/right pair of E^4 cells after the anterior pair was killed (n = 20/21; the exceptional embryo had highly abnormal intestinal polarity, but in addition had abnormal body morphogenesis and so was presumably damaged by the laser beam nonspecifically). In contrast, killing either the right pair of E^4 cells (n = 18/18; Fig. 14E) or the left pair (n = 18/18; Fig. 14F) resulted in highly abnormal and asymmetric partial intestines (Figs. 14E and 14F). Remarkably, in these experiments the E^4 descendants became polarized in the same direction they would have in normal development; the nuclei of the right E^4 descendants moved to the left, and the nuclei of the left E^4 descendants moved to the right (white arrows in Figs 14D–14F indicate the center of the embryo). In all cases, cytoplasmic granules in the cells were concentrated at the poles opposite the nuclei. The cells did not intercalate, and abnormal adherens junctions containing HMR-1 and MH27 formed ectopically between dorsal and ventral cells (Fig. 14I and data not shown). PKC-3 staining was localized within or near the border of the adherens junction (data not shown). The ectopic adherens junctions were localized invariably to the nuclear pole of the cell, as in the normal intestinal primordium. The observation that right and left cells develop opposite directions of cytoplasmic polarity in these experiments supports the hypothesis that nonintestinal cells contribute to the bilateral symmetry of the normal intestine.

DISCUSSION

The *C. elegans* intestine is an extraordinarily simple organ, containing only 20 cells. The nematode *Ascaris* has an intestine similar to that of *C. elegans* at hatching, but through subsequent cell divisions develops an intestine with over a million cells and a gross anatomy much more similar to that of some vertebrate intestines (Chitwood and Chitwood, 1974; our unpublished observations). In every case, the intestine is essentially a monolayer of epithelial cells that have apical microvilli and basal basement membranes. Most of the *C. elegans* intestine is composed of rings of only 2 cells, such that the lumen of the intestine is a canal between two opposed cells. Although the lumen of the vertebrate intestine is more complex, similar extracellular "canals" are observed in other vertebrate organs such as the bile canaliculi of the liver (Bartles, 1992; Gallin, 1997). We therefore consider it likely that the basic mechanisms *C. elegans* uses to establish polarity in its 20-cell intestine will be relevant to studies on organogenesis in more complex systems. In this paper, we have described cellular events in the formation of the intestine and shown parallels with events in the formation of a second epithelial organ, the pharynx.

Cytoskeletal Polarity in the Early Primordium

Nuclear migrations are observed in the primordia of the intestine and pharynx (our present study) and in the hypodermis (Sulston *et al.*, 1983). These migrations are one of the first visible signs of cell polarity in each of these epithelial organs. In the intestinal primordium, nuclei migrate toward a midline region containing numerous microtubules. We have shown that microtubules function in nuclear migration in the intestine, as previous studies have shown that microtubules are required for nuclear migration in the hypodermis (Williams-Masson *et al.*, 1998). Centrosomes associated with the intestinal nuclei appear to rotate toward the midline during nuclear migration, suggesting that microtubule/centrosome interactions could play a role in nuclear migration.

Centrosome/nuclear rotations have been observed in other developmental systems, such as the engagement of cytotoxic T lymphocytes with their targets in vertebrates (Serrador *et al.*, 1999). The mechanism of rotation has been studied in the early blastomeres of the *C. elegans* embryo and has been shown to require microtubule function (Hyman and White, 1987; Hyman, 1989). After the centrosomes duplicate in these blastomeres, microtubules form between the centrosomes and a fixed point on the cell membrane

irregular organization. (H) Adherens junctions in an embryo such as in D; junctions visualized by the JAM-1::GFP (see Materials and Methods). Background fluorescence is due to autofluorescence of gut granules. (I) Adherens junctions in an embryo such as shown in E or F after staining with MH27. These adherens junctions formed between dorsal cells and ventral cells (not visible in E and F) and were located at the nuclear ends of the cells (see text). (J–L) PKC-3 localization within the adherens junctions of an embryos such as shown in C. (J) MH27 staining. (K) PKC-3 staining. (L) Merge of J and K. Bar, 5 μm.

called the cortical site. A microtubule-dependent force is generated between a centrosome and the cortical site that appears to rotate the centrosome/nucleus toward the site. In the early embryonic blastomeres, a set of asymmetrically localized, cortical-associated proteins that includes PKC-3 (Izumi *et al.*, 1998) and several PAR proteins (Kemphues and Strome, 1997) establishes asymmetries that determine the position of the cortical site.

As in the early blastomeres, a duplication of centrosomes occurs in the cells of the intestinal primordium prior to centrosome movement. This duplication event is unusual since none of the intestinal cells are dividing at that time, and most never undergo cytokinesis again. However, if centrosome rotation in the intestinal cells involves some of the same biochemical machinery used by the early blastomeres, it is possible that centrosome duplication is a necessary feature of this process. The PKC-3 antiserum stains cells surfaces asymmetrically both in the early blastomeres (Izumi *et al.*, 1998) and in the intestinal primordium. Interestingly, we recently have found that antisera against each of the PAR proteins PAR-1, PAR-2, PAR-3, and PAR-6 also stain the intestinal primordium, though the specificity of these staining patterns has not yet been determined (our unpublished observations). These observations suggest there may be parallels between the polarization of cells in the intestinal primordium and the polarization of early embryonic blastomeres, and are consistent with recent studies showing that some PAR-like proteins are expressed in *Drosophila* and vertebrate epithelia (Muller and Wieschaus, 1996; Bohm *et al.*, 1997; Izumi *et al.*, 1998; Kuchinke *et al.*, 1998).

What is the function of the nuclear migration to the midline of the intestinal primordium? Nuclear migrations are observed frequently in animal development and can have roles in fertilization (Wilson, 1925), in unequal cell division (Dan, 1979; Schroeder, 1987), in changing cell shape (Tomlinson, 1985), and in the asymmetric positioning of factors that determine cell fate (Nilson and Schupbach, 1999). We do not yet know whether the nuclear migrations in the primordia of the intestine or pharynx are essential for proper organ development. However, *C. elegans* mutants defective in the genes *unc-83* or *unc-84* are viable and have incomplete nuclear migrations in the hypodermis (Sulston and Horvitz, 1981; Malone *et al.*, 1999). We consider it unlikely that nuclear migration has a general role in specifying one particular axis in epithelia, because nuclei migrate apically in the intestinal primordium, basally in the pharyngeal primordium, and laterally in the hypodermal primordium.

Our analysis of nuclear migration in the intestinal primordium suggests that the intestinal cells are likely to have polarized arrays of microtubules, as have been described in several other epithelial cell types (Lafont and Simons, 1996). Although the pharyngeal and intestinal nuclei migrate in opposite directions, this does not necessarily mean that cells in the two primordia have opposite microtubule polarities. Instead, we propose that the pharyngeal nuclei may move basally only because they are forced to do so by volume constraints as the cells become wedge-shaped. We see no evidence of centrosomal/nuclear rotation toward the basal surfaces in these cells, and cross sections through the pharynx show each nucleus in a relatively central position within the available cytoplasm of the cell. Indeed, our observations on apical vesicles suggest that the intestinal and pharyngeal primordia may transport at least this organelle in the same direction, toward the midline. The apical localization of these vesicles in the intestinal primordia is particularly striking, since other cytoplasmic components like yolk and Golgi are localized a relatively large distance away toward the basal surface. If the apical vesicles are made in the Golgi, they must subsequently be transported toward the apical surface, and this transport might require a polarized cytoskeleton. In future experiments it will be important to determine how the vesicles are localized and whether this mechanism is the same in the intestinal and pharyngeal primordia.

Membrane Separation at the Midline

The apical vesicles appear at about the same time as cells lose membrane contacts across the midline. If the apical vesicles are secreted from the midline-facing membranes, their contents might contribute to cell separation by disrupting extracellular adhesion or by altering the osmolality of the extracellular fluid. Alternatively, if the vesicles originate from the surface by endocytosis, they might function in removing adhesive molecules from the cell surface. Although we do not know whether the apical vesicles arise from endocytosis, they resemble in ultrastructure some endocytic vesicles that have been described in other systems (Gruenberg and Maxfield, 1995).

The pharyngeal and intestinal lumens do not appear to form from a random expansion of the zone of cell separation at the midline. We have shown that the pharyngeal lumen forms primarily by the gradual retraction of three specific cells (the marginal cells) from the midline of the primordium (Fig. 1B). In essence, the pharyngeal lumen forms in a "collapsed" state and does not open until late embryogenesis when the connecting muscles differentiate and contract. The intestinal lumen does not form by similar cell-specific retraction; however, the size and shape of the lumen appear to be highly regulated. Adherens junctions bordering this lumen must align in each successive anterior/posterior pair of intestinal cells, and the width of the lumen is remarkably uniform throughout the entire length of the intestine. We do not know what factors limit the width of the intestinal lumen; however, one candidate is the network of intermediate filaments that underlie the lumenal membranes.

The observation that cells separate from each other at the midline suggests that the midline membranes are no longer tightly adherent. Since cells separate at the midline before adherens junctions are recognizable in the primordia, an interesting parallel exists between the way adherens junctions form in the hypodermis, intestine, and pharynx.

Hypodermal cells are born and remain on the surface of the embryo. Therefore each hypodermal cell has one unique surface that is always free from contacts with other cells or basement membranes, and this is the surface that becomes encircled by adherens junctions. Since the intestinal and pharyngeal cells are inside the embryo, all surfaces of these cells are initially in contact with other cells or basement membranes until membrane separation occurs at the midline. If hypodermal cells have a mechanism for recognizing contact-free surfaces in positioning their adherens junctions, it is possible that the intestinal and pharyngeal cells could use a similar mechanism.

Intercalation and Organ Shape

Although the pharynx contains about four times the number of intestinal cells, the length of the intestine is very similar to the length of the pharynx. Intestinal cells are larger than pharyngeal cells; however, most of the length of the intestinal tube results from it being only two cells in circumference. Since both organs form from three-dimensional aggregates of cells, what determines the number of cells at the circumference of these organs? In the pharynx, cells become wedge-shaped so that the tips from numerous cells are in contact at the midline where adherens junctions form; when the lumen expands at the midline, these cells remain linked together. Intestinal cells do not become wedge-shaped, and so there are only four cells in contact at any point along the midline of the E^{16} primordium. Four cells, indeed, eventually link together as a ring at the anterior end of the mature intestine. Our results suggest that the other cells also have the potential to link together in rings of four, though they do not do so in normal development. In our ablation experiments on the E^4 primordium, we found that adherens junctions could form between any two intestinal cells that were in contact, with a concomitant localization of the apical marker PKC-3. We therefore propose that the only reason most intestinal cells do not normally become linked in rings of four is because they intercalate. In this view, the intercalation of the intestinal cells and their inability to become wedge-shaped are of critical importance in determining the shape of the intestine and allowing a relatively long tube to be made from so few cells.

If the positions of cells in the mature intestine are compared with their lineal origins, it is seen that the two cells that form each int ring invariably have different left/right origins. Our analysis shows that this restriction is because cells never cross the midline during intercalation. This result means that cells can intercalate vertically (dorsal/ventral), but not horizontally (left/right). Why are interactions between dorsal/ventral cells different from left/right cells in the primordium? In our study, we have observed two differences between dorsal/ventral and left/right contacts that might influence intercalation. During cell intercalation, intestinal cells develop processes that invade between adjacent cells. In the intestinal primordium, left cells and right cells contact each other along membranes that have extensive networks of microtubules. These networks presumably would have to disassemble in order for cells to extend processes diagonally across the midline, and their presence might thus inhibit at least diagonal left/right intercalation.

A second difference between dorsal/ventral and left/right contacts is in the distribution of the HMR-1 cadherin. HMR-1 has been shown to function in hypodermal cell spreading (Costa *et al.*, 1998), and we see HMR-1 concentrated at the midline of the intestinal primordium prior to intercalation. We do not know the precise localization of HMR-1 within the midline region. However, the only two midline cells that lack dorsal/ventral contacts with other intestinal cells also lack HMR-1. This observation suggests the possibility that HMR-1 is restricted to dorsal/ventral contacts between intestinal cells at the midline. HMR-1 might then be in a position to facilitate dorsal/ventral intercalation between cells.

Autonomy/Nonautonomy in Intestinal Organogenesis

We would like to know the extent to which intestinal morphogenesis is determined by the intrinsic properties of E and its descendants. We addressed this issue by isolating E either by removing, or laser-ablating, all other blastomeres. A caveat in our cell culture experiments is that development might be influenced by factors in the culture medium, and in the ablation experiments it is possible that the laser-ablated blastomeres might nevertheless contribute to development. However, our results taken together strongly suggest that E descendants have two basic properties that are intrinsic to these cells. First, E descendants can generate an apical surface. In all experiments, nuclei were positioned asymmetrically near the lumenal surface as they are in normal development. In the ablation experiments, adherens junction components and the apical marker PKC-3 were localized to a specific pole of an E descendant. Cytoplasmic components moved to the opposite pole, which would be the basal surface in normal development. However because we do not yet have molecular markers for basal or lateral differentiation, we do not know if the basal or lateral surfaces are specified properly in these experiments. The basal surfaces of the E descendants had an unusually rounded appearance (see Fig. 14), which could result from improper differentiation or simply from the lack of a substrate for adhesion. In comparison, vertebrate MDCK cells that are grown in isolation under certain culture conditions can form apical poles, but do not form proper basal–lateral domains (Vega-Salas *et al.*, 1987; Rodriguez-Boulan and Nelson, 1989).

The second basic property of the E descendants is that they are able to polarize coordinately. In our experiments, adjacent E descendants invariably had the same axis of polarity, regardless of the right/left origins of the two cells. This ability to polarize coordinately presumably is the mechanism by which the E descendants produce cyst-like

structures with radial symmetry in the isolation experiments.

Cross sections of the early E^{16} primordium in a normal embryo show a radially symmetrical arrangement of cells, analogous to the arrangement of cells in the cysts formed in our E isolation experiments. However the pattern of cell intercalation shows that the normal primordium is fundamentally bilaterally, rather than radially, symmetrical; right cells are different from left. Our laser ablation analysis of the E^4 cells provides a further demonstration of right/left differences in the intestinal primordium. In these experiments, right cells consistently polarized toward the left, and left cells polarized toward the right. Our results thus suggest that nonintestinal cells must modify the intrinsic equivalency of the E descendants to create bilateral symmetry in the intestinal primordium. These interactions could be either permissive or instructive. For example, nonintestinal cells might provide a permissive substrate for the normal cleavage pattern of E, so that left and right cells did not commingle. Indeed, we observed some abnormal cleavage planes at the E^8 to E^{16} division of an isolated E blastomere (our unpublished observations). Alternatively, nonintestinal cells might secrete specific polarizing factors on the surfaces of cells in the primordium asymmetrically.

In summary, we have shown that the principal events in intestinal organogenesis are the cytoplasmic polarization of the primordium, the separation of cell membranes at the midline, the intercalation of separate left and right sides to form a bilaterally symmetric primordium, and the formation of adherens junctions between cells of opposite polarity. There are some intriguing cytological parallels between the early events at the midlines of the intestine and pharynx, such as the localization of the apical vesicles, and it will be interesting to determine whether these events have the same molecular basis. We believe the ease of scoring intestinal cell polarity by light microscopy in living embryos, and the ability for E descendants to polarize in culture, should make the *C. elegans* intestine a very attractive system for genetic and reverse genetic analysis of epithelial morphogenesis.

ACKNOWLEDGMENTS

We thank Paulette Brunner for assistance with confocal microscopy. We are grateful for the generous gifts of strains and reagents from Jeff Hardin, Ken Kemphues, Lisa Matthews, Jeff Simske, Yo Tabuse, and Bob Waterston. We thank members of the Priess laboratory for helpful discussions, particularly Jason Pitt for the Nematode Navigator software. Some nematode strains used in this work were provided by the *Caenorhabditis* Genetic Center, which is funded by the NIH National Center for Research Resources (NCRR). B. Leung is supported by a training grant from the National Cancer Institute (CA09657-09); G. Hermann is supported by a postdoctoral fellowship from the Damon Runyon–Walter Winchell Foundation; J. Priess is supported by the Howard Hughes Medical Institute.

REFERENCES

Albertson, D. G. (1984). Formation of the first cleavage spindle in nematode embryos. *Dev. Biol.* **101,** 61–72.

Albertson, D. G., and Thomson, J. N. (1976). The pharynx of *Caenorhabditis elegans. Philos. Trans. R. Soc. (London) B* **275,** 299–325.

Babu, P. (1974). Biochemical genetics of *Caenorhabditis elegans. Mol. Gen. Genet.* **135,** 39–44.

Bartles, J. R. (1992). The establishment and maintenance of hepatocyte surface polarity. *In* "Epithelial Organization and Development" (T. P. Fleming, Ed.), pp. 219–244. Chapman & Hall, Cambridge.

Baum, P. D., and Garriga, G. (1997). Neuronal migrations and axon fasciculation are disrupted in *ina-1* integrin mutants. *Neuron* **19,** 51–62.

Bohm, H., Brinkmann, V., Drab, M., Henske, A., and Kurzchalia, T. V. (1997). Mammalian homologues of *C. elegans* PAR-1 are asymmetrically localized in epithelial cells and may influence their polarity. *Curr. Biol.* **7,** R603–R606.

Bowerman, B. (1998). Maternal control of pattern formation in early *Caenorhabditis elegans* embryos. *Curr. Top. Dev. Biol.* **39,** 73–117.

Bowerman, B., and Shelton, C. A. (1999). Cell polarity in the early *Caenorhabditis elegans* embryo. *Curr. Opin. Genet. Dev.* **9,** 390–395.

Brenner, S. (1974). The genetics of *Caenorhabditis elegans. Genetics* **77,** 71–94.

Chant, J. (1996). Generation of cell polarity in yeast. *Curr. Opin. Cell Biol.* **8,** 557–565.

Chitwood, B. G., and Chitwood, M. B. (1974). "Introduction to Nematology." University Park Press, Baltimore.

Clokey, G. V., and Jacobson, L. A. (1986). The autofluorescent "lipofuscin granules" in the intestinal cells of *Caenorhabditis elegans* are secondary lysosomes. *Mech. Ageing Dev.* **35,** 79–94.

Cobb, N. A. (1914). Rhabditin. Contribution to a science of nematology. *J. Parisitol.* **1,** 40–41.

Consortium (1998). Genome sequence of the nematode *C. elegans:* A platform for investigating biology. *Science* **282,** 2012–2018.

Costa, M., Raich, W., Agbunag, C., Leung, B., Hardin, J., and Priess, J. R. (1998). A putative catenin–cadherin system mediates morphogenesis of the *Caenorhabditis elegans* embryo. *J. Cell Biol.* **141,** 297–308.

Dan, K. (1979). Studies on unequal cleavage in sea urchins. I. Migration of the nuclei to the vegetal pole. *Dev. Growth Differ.* **21,** 527–536.

Draper, B. W., Mello, C. C., Bowerman, B., Hardin, J., and Priess, J. R. (1996). MEX-3 is a KH domain protein that regulates blastomere identity in early *C. elegans* embryos. *Cell* **87,** 205–216.

Drubin, D. G., and Nelson, W. J. (1996). Origins of cell polarity. *Cell* **84,** 335–344.

Eaton, S., and Simons, K. (1995). Apical, basal, and lateral cues for epithelial polarization. *Cell* **82,** 5–8.

Eisenmann, D. M., Maloof, J. N., Simske, J. S., Kenyon, C., and Kim, S. K. (1998). The beta-catenin homolog BAR-1 and LET-60 Ras coordinately regulate the Hox gene *lin-39* during *Caenorhabditis elegans* vulval development. *Development* **125,** 3667–3680.

Francis, G. R., and Waterston, R. H. (1985). Muscle organization in *Caenorhabditis elegans:* Localization of proteins implicated in thin filament attachment and Z-band organization. *J. Cell Biol.* **101,** 1532–1549.

Francis, R., and Waterston, R. H. (1991). Muscle cell attachment in *Caenorhabditis elegans. J. Cell Biol.* **114,** 465–479.

Gallin, W. J. (1997). Development and maintenance of bile canaliculi in vitro and in vivo. *Microsc. Res. Tech.* **39,** 406–412.

Gettner, S. N., Kenyon, C., and Reichardt, L. F. (1995). Characterization of βpat-3 heterodimers, a family of essential integrin receptors in *C. elegans. J. Cell Biol.* **129,** 1127–1141.

Graham, P. L., Johnson, J. J., Wang, S., Sibley, M. H., Gupta, M. C., and Kramer, J. M. (1997). Type IV collagen is detectable in most, but not all, basement membranes of *Caenorhabditis elegans* and assembles in tissues that do not express it. *J. Cell Biol.* **137,** 1171–1183.

Gruenberg, J., and Maxfield, F. (1995). Membrane transport in the endocytic pathway. *Curr. Opin. Cell Biol.* **7,** 552–563.

Guo, S., and Kemphues, K. J. (1996). Molecular genetics of asymmetric cleavage in the early *Caenorhabditis elegans* embryo. *Curr. Opin. Genet. Dev.* **6,** 408–415.

Gupta, M. C., Graham, P. L., and Kramer, J. M. (1997). Characterization of alpha1(IV) collagen mutations in *Caenorhabditis elegans* and the effects of alpha1 and alpha2(IV) mutations on type IV collagen distribution. *J. Cell Biol.* **137,** 1185–1196.

Hedgecock, E. M., and White, J. G. (1985). Polyploid tissues in the nematode *Caenorhabditis elegans. Dev. Biol.* **107,** 128–133.

Hyman, A. A. (1989). Centrosome movements in the early divisions of *Caenorhabditis elegans:* A cortical site determining centrosome position. *J. Cell Biol.* **109,** 1185–1193.

Hyman, A. A., and White, J. G. (1987). Determination of cell division axis in the early embryogenesis of *Caenorhabditis elegans. J. Cell Biol.* **105,** 2123–2135.

Izumi, Y., Hirose, T., Tamai, Y., Hirai, S., Nagashima, Y., Fujimoto, T., Tabuse, Y., Kemphues, K. J., and Ohno, S. (1998). An atypical PKC directly associates and colocalizes at the epithelial tight junction with ASIP, a mammalian homologue of *Caenorhabditis elegans* polarity protein PAR-3. *J. Cell Biol.* **143,** 95–106.

Kemphues, K. J., Priess, J. R., Morton, D. G., and Cheng, N. (1988). Identification of genes required for cytoplasmic localization in the early *C. elegans* embryos. *Cell* **52,** 311–320.

Kemphues, K. J., and Strome, S. (1997). Fertilization and establishment of polarity in the embryo. *In* "*Caenorhabditis elegans* II" (D. L. Riddle, T. Blumenthal, B. J. Meyer, and J. R. Priess, Eds.), pp. 335–359. Cold Spring Harbor Laboratory Press, Cold Spring Harbor, NY.

Kuchinke, U., Grawe, F., and Knust, E. (1998). Control of spindle orientation in *Drosophila* by the Par-3-related PDZ-domain protein Bazooka. *Curr. Biol.* **8,** 1357–1365.

Labouesse, M., and Mango, S. E. (1999). Patterning the *C. elegans* embryo: Moving beyond the cell lineage. *Trends Genet.* **15,** 307–313.

Lafont, F., and Simons, K. (1996). The role of microtubule-based motors in the exocytic transport of polarized cells. *Semin. Cell Dev. Biol.* **7,** 343–355.

Laufer, J. S., Bazzicalupo, P., and Wood, W. B. (1980). Segregation of developmental potential in early embryos of *Caenorhabditis elegans. Cell* **19,** 569–577.

Lin, R., Thompson, S., and Priess, J. R. (1995). *pop-1* encodes an HMG box protein required for the specification of a mesoderm precursor in early *C. elegans* embryos. *Cell* **83,** 599–609.

Madden, K., and Snyder, M. (1998). Cell polarity and morphogenesis in budding yeast. *Annu. Rev. Microbiol.* **52,** 687–744.

Malone, C. J., Fixsen, W. D., Horvitz, H. R., and Han, M. (1999). UNC-84 localizes to the nuclear envelope and is required for nuclear migration and anchoring during *C. elegans* development. *Development* **126,** 3171–3181.

Matthews, L. R., Carter, P., Thierry-Mieg, D., and Kemphues, K. (1998). ZYG-9, a *Caenorhabditis elegans* protein required for microtubule organization and function, is a component of meiotic and mitotic spindle poles. *J. Cell Biol.* **141,** 1159–1168.

Mello, C. C., Draper, B. W., Krause, M., Weintraub, H., and Priess, J. R. (1992). The *pie-1* and *mex-1* genes and maternal control of blastomere identity in early *C. elegans* embryos. *Cell* **70,** 163–176.

Moerman, D. G., Hutter, H., Mullen, G. P., and Schnabel, R. (1996). Cell autonomous expression of perlecan and plasticity of cell shape in embryonic muscle in *Caenorhabditis elegans. Dev. Biol.* **173,** 228–242.

Mohler, W. A., Simske, J. S., Williams-Masson, E. M., Hardin, J. D., and White, J. G. (1998). Dynamics and ultrastructure of developmental cell fusions in the *Caenorhabditis elegans* hypodermis. *Curr. Biol.* **8,** 1087–1090.

Muller, H.-A. J., and Wieschaus, E. (1996). *armadillo, bazooka,* and *stardust* are critical for early stages in formation of the zonula adherens and maintenance of the polarized blastoderm epithelium in *Drosophila. J. Cell Biol.* **134,** 149–163.

Newman-Smith, E. D., and Rothman, J. H. (1998). The maternal-to-zygotic transition in embryonic patterning of *Caenorhabditis elegans. Curr. Opin. Genet. Dev.* **8,** 472–480.

Nilson, L. A., and Schupbach, T. (1999). EGF receptor signaling in *Drosophila* oogenesis. *Curr. Top. Dev. Biol.* **44,** 203–243.

Pettitt, J., Wood, W. B., and Plasterk, R. H. (1996). *cdh-3,* a gene encoding a member of the cadherin superfamily, functions in epithelial cell morphogenesis in *Caenorhabditis elegans. Development* **122,** 4149–4157.

Priess, J. R., and Hirsh, D. I. (1986). *Caenorhabditis elegans* morphogenesis: The role of the cytoskeleton in elongation of the embryo. *Dev. Biol.* **117,** 156–173.

Priess, J. R., Schnabel, H., and Schnabel, R. (1987). The *glp-1* locus and cellular interactions in early *C. elegans* embryos. *Cell* **51,** 601–611.

Pruss, R. M., Mirsky, R., and Raff, M. C. (1981). All classes of intermediate filaments share a common antigenic determinant defined by a monoclonal antibody. *Cell* **27,** 419–428.

Rocheleau, C. E., Downs, W. D., Lin, R., Wittmann, C., Bei, Y., Cha, Y., Ali, M., Priess, J. R., and Mello, C. C. (1997). Wnt signaling and an APC-related gene specify endoderm in early *C. elegans* embryos. *Cell* **90,** 707–716.

Rodriguez-Boulan, E., and Nelson, W. J. (1989). Morphogenesis of the polarized epithelial cell phenotype. *Science* **245,** 718–725.

Schnabel, R., and Priess, J. R. (1997). Specification of cell fates in the early embryo. *In* "*Caenorhabditis elegans* II" (D. L. Riddle, T. Blumenthal, B. J. Meyer, and J. R. Priess, Eds.), pp. 361–382. Cold Spring Harbor Laboratory Press, Cold Spring Harbor, NY.

Schroeder, D. F., and McGhee, J. D. (1998). Anterior–posterior patterning within the *Caenorhabditis elegans* endoderm. *Development* **125,** 4877–4887.

Schroeder, T. E. (1987). Fourth cleavage of sea urchin blastomeres: Microtubule patterns and myosin localization in equal and unequal cell divisions. *Dev. Biol.* **124,** 9–22.

Serrador, J. M., Nieto, M., and Sanchez-Madrid, F. (1999). Cytoskeletal rearrangement during migration and activation of T lymphocytes. *Trends Cell Biol.* **9,** 228–232.

Shelton, C. A., and Bowerman, B. (1996). Time-dependent responses to *glp-1*-mediated inductions in early *C. elegans* embryos. *Development* **122,** 2043–2050.

Sulston, J. E., and Horvitz, H. R. (1977). Post-embryonic lineages of the nematode, *Caenorhabditis elegans. Dev. Biol.* **56,** 110–156.

Sulston, J. E., and Horvitz, H. R. (1981). Abnormal cell lineages in mutants of the nematode *Caenorhabditis elegans*. *Dev. Biol.* **82,** 41–55.

Sulston, J. E., Schierenberg, E., White, J. G., and Thomson, J. N. (1983). The embryonic cell lineage of the nematode *Caenorhabditis elegans*. *Dev. Biol.* **100,** 64–119.

Tabuse, Y., Izumi, Y., Piano, F., Kemphues, K. J., Miwa, J., and Ohno, S. (1998). Atypical protein kinase C cooperates with PAR-3 to establish embryonic polarity in *Caenorhabditis elegans*. *Development* **125,** 3607–3614.

Thorpe, C. J., Schlesinger, A. J., Carter, C., and Bowerman, B. (1997). Wnt signaling polarizes an early *C. elegans* blastomere to distinguish endoderm from mesoderm. *Cell* **90,** 695–707.

Tomlinson, A. (1985). The cellular dynamics of pattern formation in the eye of *Drosophila*. *J. Embryol. Exp. Morphol.* **89,** 313–331.

Vega-Salas, D. G., Gunderson, D., and Rodriguez-Boulan, E. (1987). Formation of the apical pole of epithelial (Madin–Darby canine kidney) cells: Polarity of an apical protein is independent of tight junctions while segregation of a basolateral marker requires cell–cell interactions. *J. Cell Biol.* **104,** 905–916.

White, J. (1988). The anatomy. *In* "The Nematode *Caenorhabditis elegans*" (W. B. Wood, Ed.), pp. 81–122. Cold Spring Harbor Laboratory Press, Cold Spring Harbor, NY.

Williams-Masson, E. M., Heid, P. J., Lavin, C. A., and Hardin, J. (1998). The cellular mechanism of epithelial rearrangement during morphogenesis of the *Caenorhabditis elegans* dorsal hypodermis. *Dev. Biol.* **204,** 263–276.

Wilson, E. B. (1925). "The Cell in Development and Heredity." Macmillan, New York.

Wu, S.-L., Staudinger, J., Olson, E. N., and Rubin, C. S. (1998). Structure, expression, and properties of an atypical protein kinase C (PKC3) from *Caenorhabditis elegans*. *J. Biol. Chem.* **273,** 1130–1143.

Yeaman, C., Grindstaff, K. K., and Nelson, W. J. (1999). New perspectives on mechanisms involved in generating epithelial cell polarity. *Physiol. Rev.* **79,** 73–98.

Zhu, J., Fukushige, T., McGhee, J. D., and Rothman, J. H. (1998). Reprogramming of early embryonic blastomeres into endodermal progenitors by a *Caenorhabditis elegans* GATA factor. *Genes Dev.* **12,** 3809–3814.

Zhu, J., Hill, R. J., Heid, P. J., Fukuyama, M., Sugimoto, A., Priess, J. R., and Rothman, J. H. (1997). *end-1* encodes an apparent GATA factor that specifies the endoderm precursor in *Caenorhabditis elegans* embryos. *Genes Dev.* **11,** 2883–2896.

Received for publication July 19, 1999
Revised August 25, 1999
Accepted August 26, 1999